Desalination and Water Treatment
www.deswater.com

doi: 10.5004/dwt.2020.25027

179 (2020) 396–417
March

Adsorption of ibuprofen from wastewater using activated carbon and graphene oxide embedded chitosan–PVA: equilibrium, kinetics, and thermodynamics and optimization with central composite design

Oya Irmak Sahin*, Berrin Saygi-Yalcin, Didem Saloglu

Engineering Faculty, Department of Chemical and Process Engineering, Yalova University, Yalova, Turkey, email: isahin@yalova.edu.tr (O.I. Sahin)

Received 18 June 2019; Accepted 14 October 2019

ABSTRACT

In the presented study, the feasibility of using activated carbon and graphene oxide embedded chitosan–poly (vinyl alcohol) (AC/CS-PVA and GO/CS-PVA) biocomposites as adsorbents for removal of ibuprofen from wastewater. The point of zero charge values, effect of AC and GO content in the biocomposites, optimum amount of biocomposites, optimum pH and ibuprofen concentration were considered. When AC and GO were embedded into CS-PVA polymer network, the ibuprofen removal performance increased from 11% to 83% and 94%, respectively. Adsorption isotherms were described by Langmuir, Freundlich, Dubinin–Radushkevich (D-R), Temkin, Halsey, Jovanovic, Elovich, and Harkins–Jura isotherm models. Freundlich, Temkin, Halsey, Elovich, and Harkins–Jura models were fitted to the adsorption better than Langmuir, D-R, and Jovanovic models. Adsorption kinetics was investigated by pseudo-first order, pseudo-second order, Elovich, Weber–Morris, and Bangham models and ibuprofen adsorption onto biocomposites represented by pseudo-second order kinetic model. The thermodynamic parameter, $\Delta H°$, $\Delta S°$, and $\Delta G°$, values were determined and the enthalpy of ibuprofen adsorption was found positive supporting the endothermic nature of pharmaceutical pollutant adsorption. The influence of various operating variables and optimum process conditions for the ibuprofen adsorption was investigated using central composite design.

Keywords: Adsorption; Activated carbon; Kinetics; Thermodynamics; Pharmaceuticals; Central composite design

1. Introduction

Pharmaceuticals and personal care products (PPCPs) are a wide range of important chemical compounds used to improve individuals' growth, health quality and hygiene. PPCPs include a wide range of products such as antibiotics, antidepressants, anti-inflammatory medications, synthetic hormones, cancer drugs, perfumes, and shampoos [1–3]. This large chemical compound class, when discarded, enters various municipal water sources such as rivers, streams, lakes, and ground water as a result of effluents from raw or treated wastewater [4–6]. Due to persistence and an undetected discharge of PPCPs in water, these compounds are defined as emerging organic environmental pollutants and have gained growing attention in recent years. Conventional wastewater treatments are insufficient to eliminate all PPCPs from water bodies [7–9]. On the contrary, modern treatments, including activated carbon adsorption, advanced oxidation and membrane processes, are more capable for the abatement of PPCPs. Beside the type of treatment, the efficiency of PPCPs removal is directly affected by the hydrophobicity and biodegradability of compounds, temperature, chemical components, and the properties of the influent [10–13].

Ibuprofen is one of the most widely consumed non-steroidal, anti-inflammatory, analgesic, and antipyretic medicines all over the world for all age groups. It has high

* Corresponding author.

mobility in aquatic environments due to its being slightly soluble in water and readily soluble in organic solvents [14,15]. A number of techniques have been developed in recent years for adsorption of ibuprofen, including ozonation, coagulation, photo-electrocatalytic degradation, ion exchange, and membrane processing. Various adsorbents, such as clay and minerals, activated clay, mats, activated carbon, carbon nanotubes, and graphene oxide, have been investigated for adsorption of ibuprofen [16–19].

A considerable amount of research has been conducted concerning the use of activated carbons (AC) used in adsorption-based technologies in the search for low-cost technologies for decontamination processes and maintaining high removal efficiencies [20,21]. Activated carbon-based technologies are a possible option to eliminate PPCPs from an aqueous medium or to act as concentrators of those pollutants for analytic purposes. Among the carbon-based materials, graphene and graphene oxide (GO) have recently received increasing attention due to their high adsorption capacities, high specific surface areas, and adaptive surface properties. GO, which has superior properties that are ideal for adsorption, is not only less expensive but also more sensitive and more reactive than other materials because of its buckled structure and hydrophilic nature with a very high negative charge density arising due to the oxygen-containing functional groups [22,23]. Considering environmental concerns, "biopolymers" have also received increasing attention for use as an absorbent for wastewater treatment. One of these adsorbent biopolymers, chitosan (CS) is biocompatible, biodegradable, non-toxic and formed in a hydrogel structure [24]. Even though CS and its derivatives have been widely applied in chemical processes; CS has weak mechanical properties such as flexibility, poor solubility, and swelling ratio. To mitigate the disadvantages of CS, auxiliary biocomposites are needed, which have to be biocompatible, low-cost, and chemically stable. Polyvinyl alcohol (PVA) is the first material to come to mind to be used for biocompatibility and an excellent hydrophilicity property of CS.

The present study considered uniting CS, PVA, AC, and GO to work together in the removal of pharmaceutical compounds from wastewater. CS-PVA biocomposites, embedded with AC and GO separately, were synthesized for the adsorption evaluation of the PPCP, ibuprofen. The main aim and the originality of the current work are to test the adsorption behavior of AC- and GO-embedded CS-PVA biocomposites for removing ibuprofen from wastewater. In this way, the effects of temperature, pH, initial ibuprofen concentration, and the amount of biocomposite in the adsorption process were evaluated and equilibrium, kinetics, thermodynamics, and optimization studies (CCD) were obtained. It can be safely mentioned that this paper represents the first example in the literature to research ibuprofen adsorption onto AC- and GO-embedded CS-PVA biocomposites.

2. Materials and methods

2.1. Materials

CS (deacetylation, DD: 85%; Mw: 100,000–300,000 Da) and PVA degree of hydrolysis: 98%; Mw: 89,000–98,000) were supplied by Sigma-Aldrich Chemical Co., (Steinheim, Germany) and used as received. All other chemicals, that is, glacial acetic acid, glutaraldehyde solution (25 wt.%) were obtained from Merck (Darmstadt, Germany). Also activated carbon graphene oxide and ibuprofen were purchased from Sigma-Aldrich Chemical Co., (Steinheim, Germany).

2.2. Preparation of CS-PVA; AC/CS-PVA, and GO/CS-PVA

AC/CS-PVA and GO/CS-PVA biocomposites were prepared in two steps using the CS-PVA preparation followed by chemical crosslinking with glutaraldehyde (GA). First, deacetylated chitosan was dissolved in deionized water containing 2% (w/w) acetic acid and stirred for 12 h to obtain a 5% (w/v) chitosan solution. PVA solution (5%, w/w) was dissolved in distilled water. Chitosan and PVA solutions were mixed in 1:1 (w/w) ratio and stirred overnight at 60°C to obtain a homogeneous CS-PVA solution. Then, 25% glutaraldehyde (GA) solution was added into the CS-PVA mixture to make a 2% (w/w) of total solution and kept under stirring for 24 h to crosslink the CS-PVA and GA. CS-PVA was washed with distilled water for removal of unreacted compounds, dried at room temperature and further dried in freeze-dryer.

AC/CS-PVA and GO/CS-PVA biocomposites were prepared with different AC:CS-PVA and GO:CS-PVA ratios of 1.0–5.0 (w/w). AC and GO with defined weight fractions were added into CS-PVA solution and the mixtures were dispersed until complete dissolution to make a homogenous mixture. Then, GA solution was added to the AC/CS-PVA and GO/CS-PVA mixture. After crosslinking, biocomposites were washed with distilled water for removal of unreacted compounds, dried at room temperature and further dried in freeze-dryer [25]. The biocomposites were coded as AC/CS-PVA:(1.0–5.0) and GO/CS-PVA:(1.0–5.0). The schematic reaction mechanism is represented in Fig. 1.

2.3. Preparation and determination of ibuprofen

Ibuprofen stock solution was prepared using methanol and ibuprofen concentration was detected using UV–Vis spectrophotometer Shimadzu UV-1800, Tokyo, Japan at 225 nm wavelength in methanol [26]. The UV absorption spectra of the ibuprofen solution prepared at 2–100 mg/L was recorded against methanol and the spectrum was obtained. Calibration graph was linear in the range 2–100 mg/L ibuprofen. Also, each experiment was duplicated under identical conditions and average results were reported.

2.4. Characterization of CS-PVA, AC/CS-PVA, and GO/CS-PVA

The molecular structure of the raw CS-PVA, AC/CS-PVA, and GO/CS-PVA was defined by a Shimadzu IR Affinity Spectrometer. The spectra were recorded by 16 scans with a resolution of 2 cm^{-1}. N_2 adsorption measurements were performed using a Micromeritics ASAP 2020 (Norcross, GA, USA) surface analyser. The specific surface area and pore volumes were obtained from nitrogen adsorption data at 77 K and surface areas were calculated by the Brunauer–Emmett–Teller (BET) method. Purging was continued for 24 h prior to analysis and the experiments were done in duplicates. The morphology of the adsorbents was examined by scanning electron microscopy (ESEM-FEG/EDAX Philips XL-30

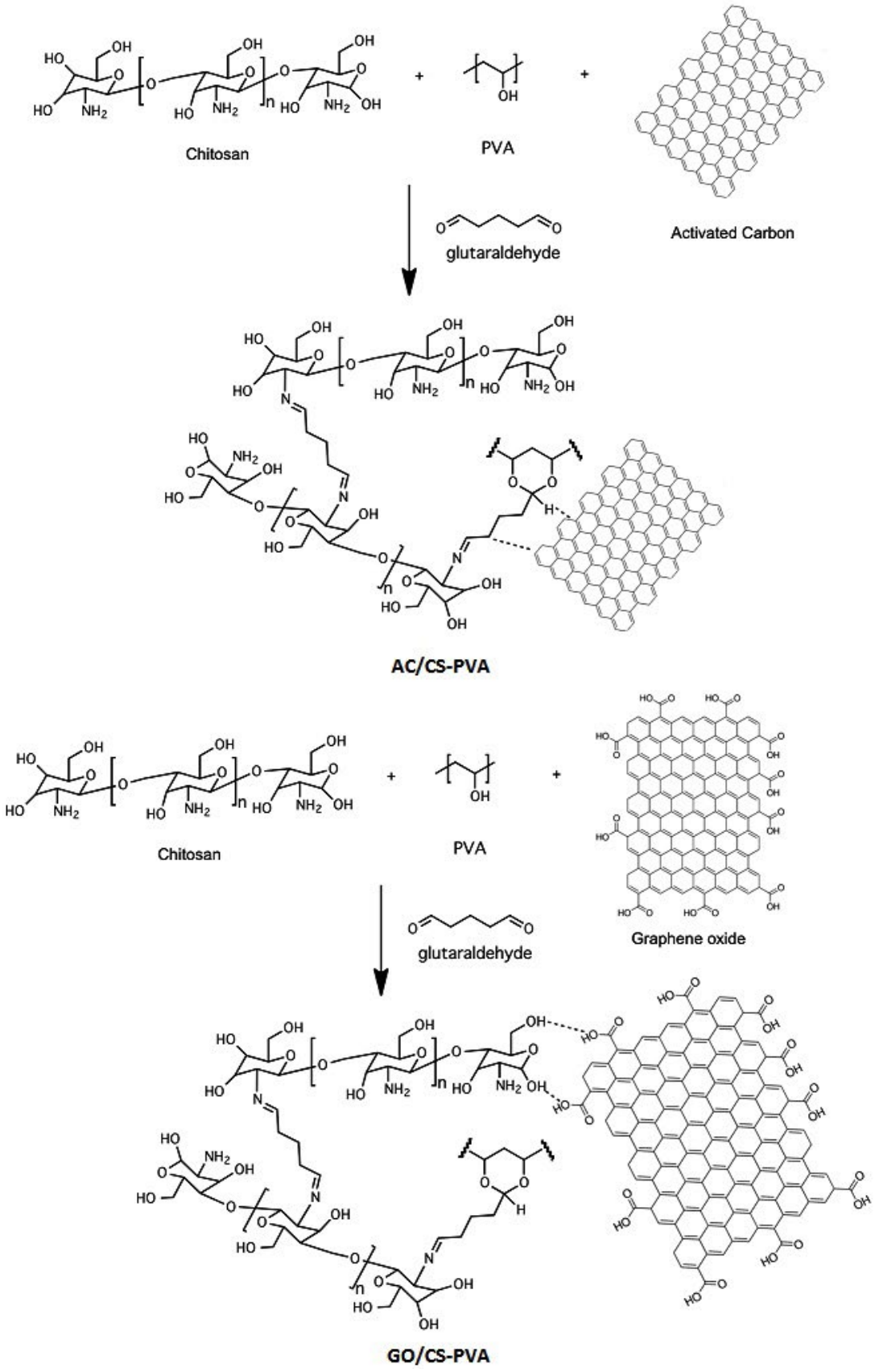

Fig. 1. Schematic reaction mechanism of AC/CS-PVA and GO/CS-PVA.

Philips, Eindhoven, Netherlands) [27,28]. The points of zero charges (PZC) of adsorbents were estimated using salt addition method. For the determination of PZC, 50 mL of 0.01 M NaCl solutions were introduced to Erlenmeyer and 0.5 g of adsorbents were taken in the Erlenmeyer, then pH values of these solutions were adjusted in 2–12 range by 0.1 M HCl/NaOH solutions and pH values were recorded as initial pH. The flasks were kept for 48 h and the final pH of the solutions was detected. Graphs were plotted between $pH_{initial}$ vs. $pH_{final-initial}$. The point of the $pH_{initial}$ = 0 was determined as PZC values of the adsorbents.

2.5. Batch adsorption experiments

In batch adsorption experiment, 25 mL of 40–100 mg/L ibuprofen solutions in methanol with pH from 3.0 to 11.0, by dropping 0.1 M HCl/NaOH solutions, were added to 20–100 mg of AC/CS-PVA:(1.0–5.0) and GO/CS-PVA:(1.0–5.0) biocomposites in a 250 mL Erlenmeyer at 20°C–60°C ± 0.5°C; and adsorption experiment was performed on a mechanical shaker at 140 rpm during 180 min. Then the biocomposites were separated from solution and absorbance values of the supernatants were measured. Each experiment was duplicated under identical conditions and average results were reported.

Eq. (1) is used to calculate the adsorption capacity of ibuprofen [28]:

$$q_e = \frac{\left(C_i - C_e\right) \times V}{m} \tag{1}$$

q_e is adsorption capacity (mg/g), V is volume (L), m is amount of adsorbent (g), C_i and C_e are initial and equilibrium concentrations (mg/L), respectively.

2.6. Adsorption isotherms, kinetics, and thermodynamics

Adsorption isotherms of adsorbed ibuprofen onto raw CS-PVA, raw AC, raw GO, AC/CS-PVA, and GO/CS-PVA were described by Langmuir, Freundlich, Dubinin–Radushkevich (D-R), Temkin, Halsey, Javanovic, Elovich, Harkins–Jura models [29]. The isotherms were studied using 40 mg/L ibuprofen solution in methanol with 20–100 mg of biocomposites at pH 3.0.

Kinetic experiments were carried out using 40 mg/L ibuprofen solution with defined amount of biocomposites and the adsorption kinetics were investigated by pseudo-first order, pseudo-second order, Elovich, Weber–Morris, and Bangham models [30].

Adsorption experiments were carried out for 303, 313, 323, and 333 K at pH 3.0, ibuprofen concentration 40 mg/L and contact time 180 min to examine the adsorption thermodynamics [31]. The thermodynamic parameters were calculated from the following equations:

$$\ln \frac{q_e}{C_e} = \frac{\Delta S^\circ}{2.303R} - \frac{\Delta H^\circ}{2.303RT} \tag{2}$$

$$\Delta G^\circ = \Delta H^\circ - T\,\Delta S^\circ \tag{3}$$

where R is gas constant (8.314 J/mol K) and T is the absolute temperature (K).

2.7. Experimental design and data analysis

A five level and four variable central composite designs were applied to optimize the adsorption process for ibuprofen. The coded and actual levels of experimental variables, pH (3.0–11.0), temperature (20°C–60°C), amount of biocomposites (20–100 mg) and initial ibuprofen concentration (20–100 mg/L), were given in Table 1 is used for optimization of the adsorption processes. Experimental design and statistical analysis were performed with the aid of software Design-Expert (Stat-Ease Inc, Minneapolis, MN). The experimental design matrix for actual process variables and responses (removal percentage of Ibuprofen for AC and GO adsorbents) is listed in Table 2.

3. Results and discussion

3.1. Characterization of CS-PVA; AC/CS-PVA, and GO/CS-PVA

FT-IR analysis is employed to detect the interactions between CS-PVA, AC and GO. Fig. 2 presents the FT-IR spectra for all adsorbents. The peaks at 3,300; 1,650; and 1,400–1,000 cm^{-1} for GO are attributed to the O–H, C=O in COOH, and C–O in COH/COC groups, respectively [17]. Strong absorption peak of graphene oxide at 1,650 cm^{-1} is stretching vibration of benzene ring skeleton. Also, from the FTIR spectra of AC, the weak absorption peaks at 1,580 cm^{-1} indicate the presence of aromatic C=C groups. Whereas, the absorption peak at 1,082 cm^{-1} is attributed to C–O–H group. As shown from FTIR spectra for CS-PVA, the broad band with a maximum force near 3,300 cm^{-1} corresponds to –OH and N–H stretching's, as well as the intramolecular

Table 1
Levels of experimental variables

Independent variable	Coded	Range	Levels of variables				
			–2	–1	0	+1	+2
pH	*A*	3.0–11.0	3.0	5.0	7.0	9.0	11.0
Temperature (°C)	*B*	20–60	20	30	40	50	60
Amount of biocomposite (mg)	*C*	20–100	20	40	60	80	100
Ibuprofen concentration (mg/L)	*D*	20–100	20	40	60	80	100

Table 2
Experimental design matrix with experimental data

	Actual values of variables				Responses	
	pH	Temperature (°C)	Amount of biocomposite (mg)	Concentration (mg/L)	Removal % (AC/CS-PVA:3.0)	Removal % (GO/CS-PVA:3.0)
1	9.0	50	80	80	50	58
2	7.0	40	60	60	68	78
3	5.0	30	80	40	68	80
4	9.0	30	40	80	30	44
5	7.0	40	60	20	64	84
6	9.0	50	40	80	39	58
7	3.0	40	60	60	82	79
8	7.0	60	60	60	78	94
9	9.0	30	80	80	34	46
10	9.0	30	40	40	15	50
11	5.0	30	40	40	65	65
12	7.0	40	60	100	59	70
13	7.0	40	20	60	51	64
14	7.0	40	60	60	68	78
15	5.0	50	80	80	76	91
16	9.0	50	40	40	28	63
17	9.0	50	80	40	41	71
18	9.0	30	80	40	30	60
19	7.0	40	60	60	68	78
20	7.0	40	60	60	68	78
21	5.0	30	40	80	48	74
22	5.0	50	80	40	83	93
23	11.0	40	60	60	34	32
24	7.0	40	60	60	68	78
25	5.0	30	80	80	60	78
26	7.0	40	100	60	77	91
27	5.0	50	40	80	52	83
28	7.0	20	60	60	45	61
29	5.0	50	40	40	78	87
30	7.0	40	60	60	68	78

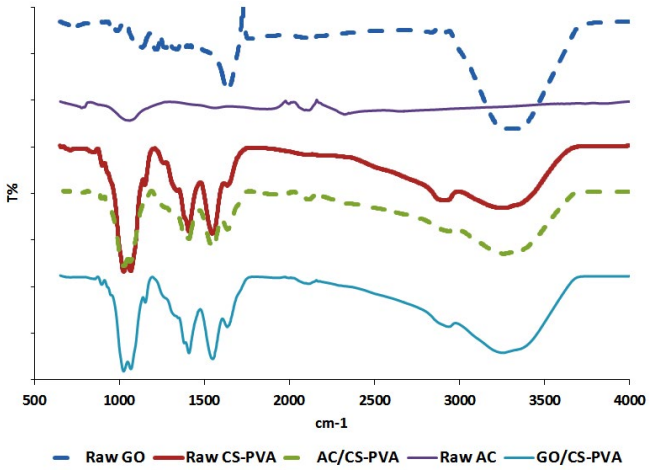

Fig. 2. FT-IR spectra of CS-PVA, AC/CS-PVA and GO/CS-PVA.

hydrogen bindings and the band at 2,950 cm^{-1} is attributed to C–H bond. The broad peak at 1,650 cm^{-1} is confirmed by C=N bond formed by the reaction of amino group of chitosan and aldehyde groups from glutaraldehyde as a crosslinker. The adsorption peak at 1,080 cm^{-1} indicates N–H stretching vibration [27].

Several spectacular differences appeared in the FT–IR spectra of AC/CS-PVA and GO/CS-PVA biocomposites in comparison with raw CS-PVA, raw AC and raw GO. In the FTIR spectra of GO/CS-PVA, the peaks at near 3,300 cm^{-1} shows the N–H and O–H vibration of chitosan, PVA, and GO. The weakened intensity at 1,650 cm^{-1} possibly explained the interaction of COOH groups of GO and O–H groups of CS-PVA. Also, the strong peaks between 1,000 and 1,400 cm^{-1} explained by interaction between the COH/COC groups of GO and N–H groups of CS-PVA. It is clear from the FT-IR spectrum of the AC/CS-PVA, the strong peak at 3,300 cm^{-1} is probably caused by an interaction between AC and O–H

and N–H groups of CS-PVA. Also, the reduced intensity of absorption peak at 1,580 cm^{-1} belongs to C=C group is probably caused by an interaction between AC and O–H groups. Strong absorption bands between 1,000 and 1,400 cm^{-1} were explained by interaction of C–O–H group of AC and N–H groups of CS-PVA. In the FT-IR spectra of AC/CS-PVA and GO/CS-PVA, the peaks at 2,950 cm^{-1} is attributed to C–H stretch, the most abundant functional groups available in CS-PVA. So, by comparing the spectrum with the FT-IR spectra of the AC and GO, it is revealed that the CS-PVA has been supported with AC and GO. Thus, for AC/CS-PVA and GO/CS-PVA biocomposites, the FTIR spectra confirmed the appropriateness of the AC and GO embedding processes into the CS-PVA.

Adsorption is a surface reaction and is significantly affected by physical properties such as surface area, pore structure, and particle size of the adsorbent. An adsorbent with a high surface area can trap more adsorbate molecules on its surface, thereby increasing its adsorption capacity. Also, another important parameter that guides the adsorption mechanism is the pore structure. The pore structure of the adsorbent refers to the size of the pores and the pore size distribution. In this work, according to the explanation about the adsorbent surface properties, SEM and BET analyses were investigated to determine the efficiency and adsorption capacity of the AC/CS-PVA and GO/CS-PVA.

The SEM images of raw CS-PVA, AC/CS-PVA, and GO/CS-PVA of the surface are shown in Fig. 3. It can be can observed clearly that raw CS-PVA shows essentially the undeveloped porous surface morphology composed of randomly distributed small closed pores with a pore size of 3–5 micrometers with a lot of interstices. Also, there are protrusions and reticulated structures extending from the surface of CS-PVA. It seems clearly that, the surfaces of CS-PVA changed after modification with AC and GO having a fine three-dimensional network structure and resulted in a surface with porous structure. Pore size of AC/CS-PVA biocomposite was in the range of 8–10 micrometer and more

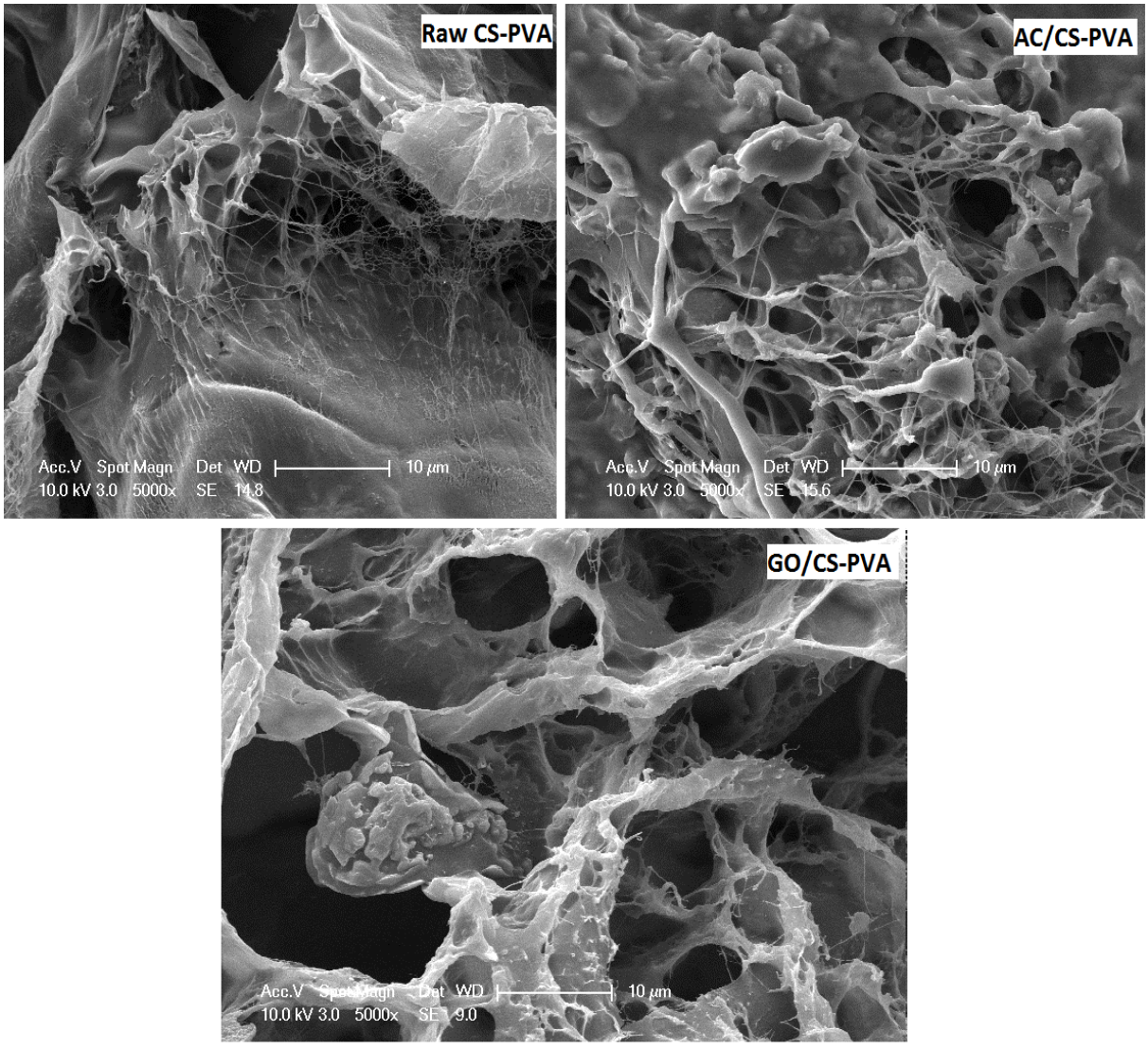

Fig. 3. SEM images of CS-PVA, AC/CS-PVA and GO/CS-PVA.

cavities were exposed to the surface. However, when compared with CS-PVA, the pore size of AC/CS-PVA was larger, the number of round pores was higher and AC/CS-PVA had a different distribution of the cavities on the surface. This may explain the higher AC embedding capacity of the CS-PVA. Likewise, larger pore size can be observed in GO/CS-PVA and SEM image for GO/CS-PVA suggests that the increase of GO incorporation resulted in increase of porosity; pore size was in the range of 20–40 micrometers, and not round shapes were observed. From SEM images of GO/CS-PVA, nonhomogenous pore distribution and larger cavities formation, compared with CS/PVA and AC/CA-PVA, were seen. The cavities of GO/CS-PVA appeared larger than AC/CS-PVA and SEM images showed bigger and non-round cavities when compared with AC/CS-PVA and CS-PVA.

These results can be accepted as an indication of the successful embedding of AC and GO. The presence of AC/CS-PVA and GO/CS-PVA porous network structure where all potential binding sites are under receptive position was found to be responsible for the dramatic increase in the ibuprofen adsorption. On the basis of the comparison between the SEM images of the AC- and GO-embedded CS-PVA, it can be concluded that the porous structure greatly facilitates the biocomposites in the removal of ibuprofen directly.

The BET analysis of the biocomposites is given in Table 3 and the table represents the effect of AC and GO on the specific average surface area and pore volume of AC/CS-PVA and GO/CS-PVA. The specific surface areas for the raw CS-PVA, raw AC, raw GO, AC/CS-PVA, and GO/CS-PVA were 2.19, 429.8, 736.3, 224.5, and 356.9 m^2/g, respectively. However, CS-PVA exhibited the least specific surface area while GO has the highest and the biocomposites resulted in a larger surface area than that of CS-PVA. The specific surface area was in the order of GO > AC > GO/CS-PVA > AC/CS-PVA > CS-PVA. Also total pore volume values were increased with embedding AC and GO into the CS-PVA. GO showed larger total pore volume, indicating that larger pores were formed in the GO/CS-PVA. The total pore volume values were determined as 0.0058 and 0.0034 cm^3/g for GO/CS-PVA and AC/CS-PVA, respectively. It can be safely stated that the improvement of the surface properties of the CS-PVA occurred by AC and GO acting as a supporting material.

The point of zero charge (PZC) for an adsorbent surface is the pH at which that surface has a net neutral charge. The adsorbent surface is positively charged at a solution pH less than the PZC, and thus it can be an adsorbent surface for anions. On the contrary, when it is negatively charged at a solution pH higher than the PZC, the adsorbent surface can absorb cations [32]. The point of zero charge for the adsorbent surfaces is given in Fig. 4. The raw CS-PVA sample had a positive surface charge at a pH lower than 8.0 owing to the presence of amino groups belong to chitosan; also, the PZC value of raw AC and raw GO was found as 7.0 and 4.2, respectively. The PZC values were determined as 7.5 for AC/CS-PVA:(1.0–5.0) and 6.5 for GO/CS-PVA:(1.0–5.0) biocomposites. When compared with raw CS-PVA, the PZC values of biocomposites decreased after embedding both AC and GO due to the hydrogen bonding between the CS-PVA, AC, and GO. Also, AC/CS-PVA and GO/CS-PVA, consisting of both cationic and anionic functional groups, can be applied for treatment of wastewater including ibuprofen.

Table 3
BET analysis results of biocomposites

	Total pore volume (cm^3/g)	Average specific surface area (m^2/g)
CS-PVA	<0.0001	2.19
AC	0.221	429.8
GO	0.378	736.5
AC/CS-PVA	0.0034	224.5
GO/CS-PVA	0.0058	356.9

3.2. Determination of AC and GO content, optimum amount of biocomposites, pH and ibuprofen solution concentration

Fig. 5 displays the removal percentages of ibuprofen using raw CS-PVA, raw AC, raw GO, AC/CS-PVA:(1.0–5.0), and GO/CS-PVA:(1.0–5.0) biocomposites as an adsorbent. The ibuprofen adsorption capacity (q_e) values were determined as 18.5 and 19.5 mg/g for raw AC and GO, respectively. Also, q_e values were calculated as 11.6; 15.0, and 15.5 using AC/CS-PVA:(1.0, 3.0, and 5.0) as an absorbent and 12.3; 17.0; and 18.2 mg/g using GO/CS-PVA:(1.0, 3.0, and 5.0), respectively. Removal percentage values were detected as 58%, 75%, 78% and 62%, 87%, 91%, using 1.0%–5.0% (w/w) AC- and GO-embedded biocomposites, respectively. It can be concluded that as AC and GO content increased from 1.0 to 5.0 (w/w), ibuprofen adsorption removal percentages were boosted dramatically from 58% to 78% for AC/CS-PVA and from 62% to 91% for GO/CS-PVA. In addition, q_e values were estimated as 15.0 and 17.0 mg/g; removal percentages were calculated as 75% and 87% using AC/CS-PVA:3.0 and GO/CS-PVA:3.0, respectively. According to the results from Fig. 5, q_e and removal % values belonging to AC/CS-PVA:3.0&5.0 and GO/CS-PVA:3.0&5.0 were very close to each other. Thus, 3.0% (w/w) AC and GO contents in the biocomposite were used as the optimum content of AC and GO in the CS-PVA for experiments testing the effect of biocomposite amounts.

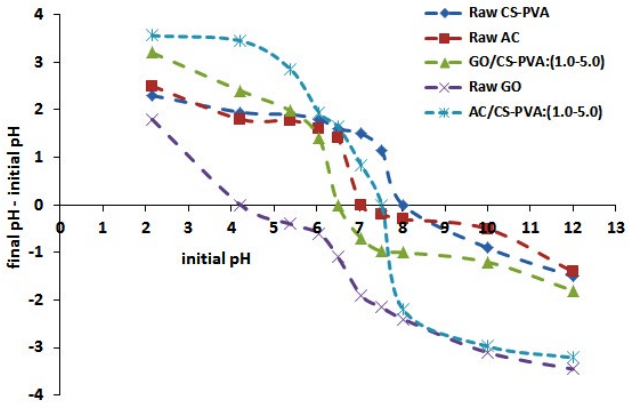

Fig. 4. The point of zero charge for the adsorbent surfaces.

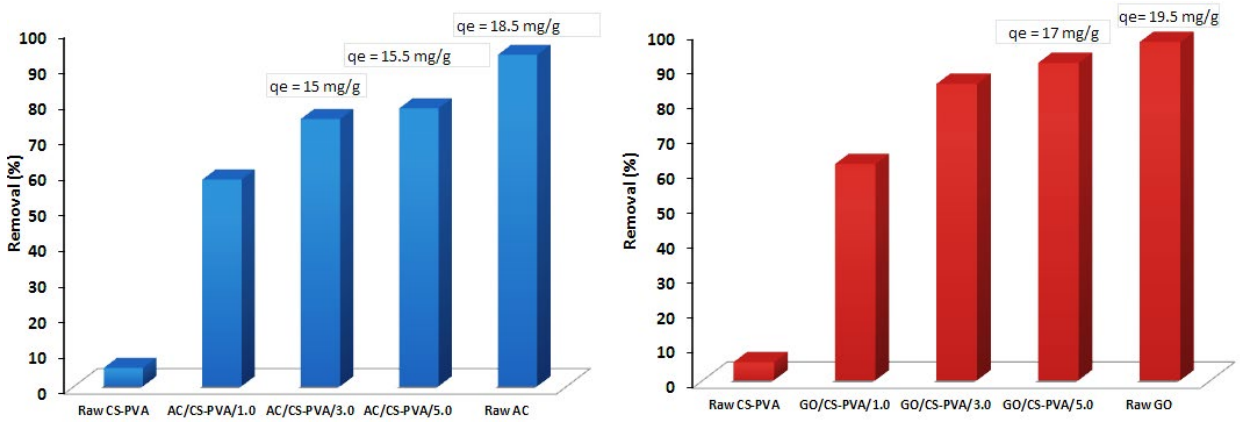

Fig. 5. Adsorption capacity and removal percentages of ibuprofen using biocomposites with different AC and GO content.

The effect of biocomposite amount on the ibuprofen adsorption was investigated in the range of 20 to 100 mg of biocomposite for 40 mg/L ibuprofen solution (Fig. 6). The adsorption removal percentages increased with an increasing in amount of biocomposites. As the biocomposite quantity increased from 20 to 100 mg, the removal % values were raised from 55% to 75% and 67.5% to 85%, despite q_e values being slightly decreased from 65.5 to 17.1 mg/g and 55.0 to 18.3 mg/g using AC/CS-PVA:3.0 and GO/CS-PVA:3.0, respectively. As can be seen from Fig. 6, amount of AC/CS-PVA:3.0 and GO/CS-PVA:3.0 affected the ibuprofen adsorption with similar trends. Hence, 100 mg of each of adsorbents were preferred as the optimum amount of biocomposite and 100 mg of biocomposite was applied for following the pH effect on the ibuprofen adsorption experiments.

The effect of pH on ibuprofen adsorption from 40 to 100 mg/L ibuprofen solution using 3.0% AC- and GO-embedded CS-PVA is shown in Fig. 7. The results indicated that the ibuprofen adsorption capacities of both AC/CHT-PVA:3.0 and GO/CS-PVA:3.0 decreased significantly with rising pH from 3.0 to 11.0. It can be followed from the figure that; the removal percentages of ibuprofen were higher at acidic and neutral pHs than basic pH values. At pH 3.0, the maximum removal percentage values were at nearly 75% for AC/CS-PVA:3.0 and 85% for GO/CS-PVA:3.0 in 40 mg/L ibuprofen solution. Also, the removal percentage for AC/CS-PVA:3.0 decreased from 75% to 35% with an increasing pH value from 3.0 to 11.0, while it increased from 55% to 85% from pH 11.0 to pH 3.0 for GO/CS-PVA:3.0.

The plausible explanation of the pH effect might be that AC/CS-PVA and GO/CS-PVA consisting of hydrogen, hydroxyl, carbonyl, aldehyde, amine and carboxyl groups can be applied for adsorption of ibuprofen in acidic and neutral pH values due to these anionic and cationic groups affecting the interactions between the biocomposites and ibuprofen. In addition, considering the dissociation of ibuprofen (nearly pKa: 5.0) [33], it presents in solution a negative charge over pH 5.0. Thus, between pH 5.0 and PZC of the biocomposite surface ($PZC_{AC/CS-PVA}$ = 7.5 and $PZC_{GO/CS-PVA}$ = 6.5), ibuprofen molecules can be adsorbed effectively by π–π interactions, the hydrophilic–hydrophobic interactions and the electrostatic interactions. Moreover, at pH 9.0 and 11.0, the repulsion of ibuprofen and the dissociation of

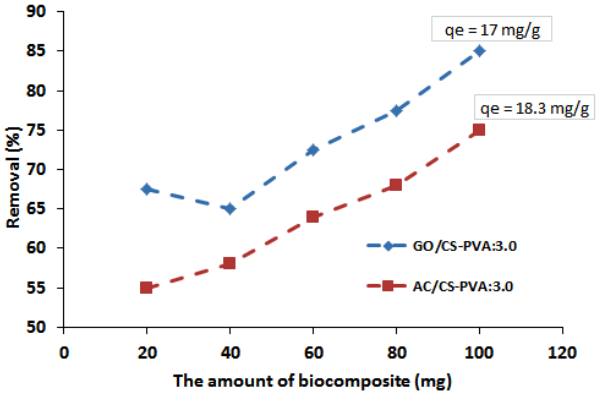

Fig. 6. Effect of amount of biocomposite on ibuprofen adsorption.

functional groups of biocomposites were established resulting in a decrease in the interaction. Since the superficial charge of biocomposites was negative above pH 6.5, when the pH increased to 9.0, the electrostatic repulsion force occurred and –OH ions in the solution competed with ibuprofen anions to gain the sorption active sites and this competition decreased the adsorption efficiency. It can be concluded that when pH values were 3.0 and 5.0 the surfaces of the biocomposites became positively charged, which began to adsorb –OH groups belonging to ibuprofen through the electrostatic force of attraction. The maximum adsorption rates were obtained below neutral and acidic pH values as positive charge surfaces of both AC/CS-PVA:3.0 and GO/CS-PVA:3.0. Therefore, pH 3.0 was selected as the optimum pH value for ibuprofen adsorption. Fig. 7 also indicates the effect of ibuprofen solution concentration on adsorption. It was found that the ibuprofen removal percentage decreased from 75% to 65% and 85% to 63% using AC/CS-PVA:3.0 and GO/CS-PVA:3.0, respectively, with an increase in ibuprofen concentration from 40 to 100 mg/L at pH 3.0. In addition to this, the removal percentages decreased from 73% to 53% using AC/CS-PVA:3.0 and from 85% to 63% using GO/CS-PVA:3.0 in an ibuprofen concentration range between 40 and 100 mg/L at pH 5.0 and also the adsorption removal percentages of both AC/CS-PVA and GO/CS-PVA showed a similar downward trend at 7.0. However, q_e values attained

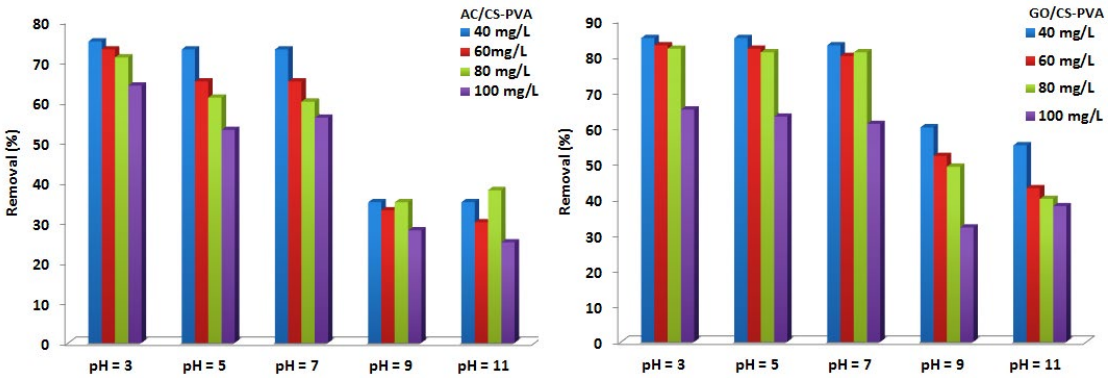

Fig. 7. Effect of pH and ibuprofen solution concentration (mg/L) onto adsorption (a) AC/CS-PVA:3.0 and (b) GO/CS-PVA:3.0.

maximum at 18.3 mg/g for 40 mg/L, 22.1 mg/g for 60 mg/L, 29.7 mg/g for 80 mg/L, and 32.3 mg/g for 100 mg/L ibuprofen solution, using AC/CS-PVA:3.0 at pH 3.0. The q_e values for GO/CS-PVA:3.0 were determined as 17.1 mg/g for 40 mg/L, 22.8 mg/g for 60 mg/L, 29.4 mg/g for 80 mg/L and 32.1 mg/g for 100 mg/L ibuprofen solution at the same pH value.

The reason for this behavior is attributed to the saturation of adsorption sites. Saturation of active sites is a case in which adsorbed phase volume is totally filled with adsorbate and the density of the adsorbed phase reaches maximum. When surface excess is adsorbate molecules in the adsorbed phase, lowered by the adsorbate amount that would attend the same adsorbed phase, then adsorption cannot occur effectively [34]. Therefore, active sites of the AC/CS-PVA:3.0 and GO/CS-PVA:3.0 were totally filled and closed with ibuprofen molecules at low concentrations (40 and 60 mg/L), so adsorption efficiency declined significantly with an increasing ibuprofen concentration.

Considering all preliminary adsorption experiments, the plausible adsorption mechanism between ibuprofen and AC- and GO-embedded CS-PVA biocomposites can be explained with characteristics of carbonaceous adsorbents. Two important factors affect the ibuprofen adsorption: hydrogen-bond interaction between the biocomposites and ibuprofen molecules and π–π interactions between π electrons of ibuprofen and π electrons of benzene rings of carbonaceous biocomposites [25,27]. As ibuprofen molecule has a benzene ring [15], the essential intermolecular force between ibuprofen and GO/CS-PVA biocomposites might be the π–π interaction. In addition, Simsek et al. [25] introduced that hydrogen bonding between OH group in both ibuprofen and AC- and GO-embedded CS-PVA biocomposites could be involved in the adsorption reaction.

In the present study, according to the point of zero charge values, the effect of AC and GO content in the biocomposites, the amount of biocomposites, the pH and the ibuprofen concentration onto adsorption; equilibrium studies; adsorption isotherms; adsorption kinetics; and the thermodynamic study of ibuprofen were conducted with AC/CS-PVA:3.0 and GO/CS-PVA:3.0 biocomposites.

3.3. Adsorption isotherms

The relationship between the ibuprofen adsorption and the equilibrium concentrations are defined by the following models: Langmuir [29], Freundlich [35], Dubinin–Radushkevich (D–R) [36], Temkin, Halsey [37], Jovanovic [36], Elovich [38], and Harkins–Jura [39]. The linearized form of the isotherm equations is followed from Table 4. Model parameters can be obtained from the slope and intercept of the related plots.

Also, Fig. 8 and Table 5 represent the adsorption isotherm parameters and correlation coefficients (R^2) of ibuprofen adsorption onto raw CS-PVA, raw AC, raw GO, AC/CS-PVA:3.0 and GO/CS-PVA:3.0.

Table 4
Adsorption isotherm model equations

Langmuir isotherm model	$\frac{1}{q_e}=\frac{1}{q_m K_L}\frac{1}{C_e}+\frac{1}{q_m}$ $R_L=\frac{1}{\left(1+C_e K_L\right)}$
Freundlich isotherm model	$q_e=K_F C_e^{\frac{1}{n}}$
Temkin isotherm model	$q_e=\frac{RT\ln\left(K_t C_e\right)}{b}$
Dubinin–Radushkevich (D–R) isotherm model	$\ln q_e=\ln q_m-\beta\left(\text{epsilon}\right)^2$ $\left(\text{epsilon}\right)=RT\ln\left(1+\frac{1}{C_e}\right)$ $\text{Energy}=\frac{1}{\sqrt{2\beta}}$
Halsey isotherm model	$q_e=\frac{1}{n_H}\ln K_H-\frac{1}{n_H}\ln C_e$
Jovanovic isotherm model	$\ln q_e=\ln q_m-K_J C_e$
Elovich isotherm model	$\ln\frac{q_e}{C_e}=\ln K_E-\frac{q_e}{q_m}$
Harkins–Jura isotherm model	$\frac{1}{q_e^2}=\frac{B}{A}-\left(\frac{1}{A}\right)\log C_e$

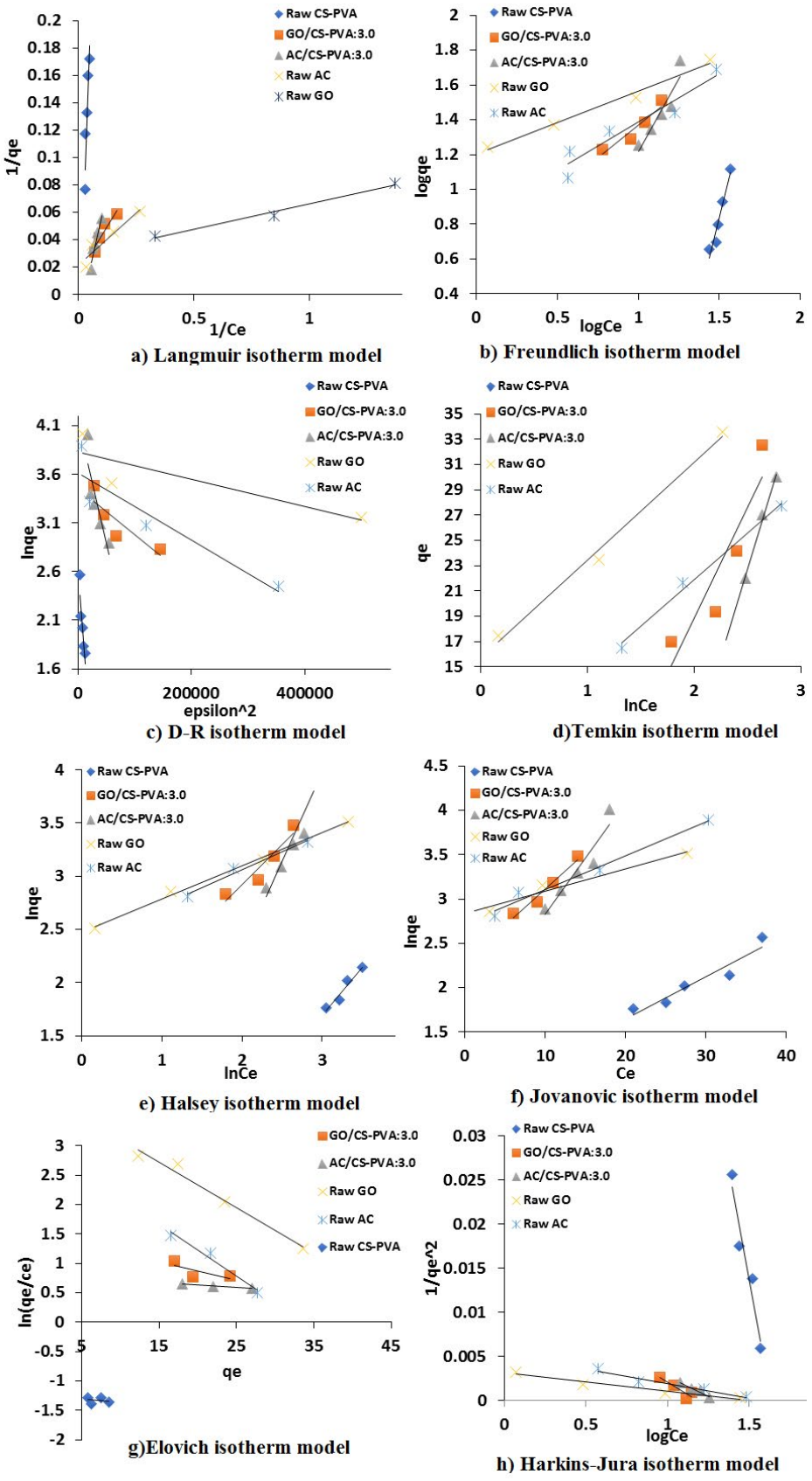

Fig. 8. Adsorption isotherms of ibuprofen.

Table 5
Adsorption isotherm model parameters of ibuprofen adsorption

	Raw CS-PVA	Raw GO	Raw AC	AC/CS-PVA:3.0	GO/CS-PVA:3.0
$q_{e,exp}$ (mg/g)	5.8	11.5	12.8	10.0	17.0
Langmuir isotherm model					
$q_{m,theo}$ (mg/g)	36.49	45.45	45.45	52.35	66.67
K_L (L/mg)	0.0062	0.514	0.142	0.025	0.054
R_L	0.80	0.15	0.046	0.50	0.32
R^2	0.89	0.96	0.91	0.92	0.87
Freundlich isotherm model					
K_F (mg/g)	25.70	15.84	6.60	2.09	4.07
$1/n$	3.72	0.362	0.557	1.69	0.75
R^2	0.93	0.98	0.92	0.96	0.90
Dubinin–Radushkevich (D–R) isotherm model					
$q_{m,theo}$ (mol/g)	45.60	36.96	45.60	62.80	31.50
β (mol^2K/J^2)	1×10^{-6}	3×10^{-6}	8×10^{-5}	2×10^{-5}	5×10^{-5}
Energy (J/mol)	79.05	408.24	707.10	158.43	100.58
R^2	0.78	0.85	0.75	0.76	0.74
Temkin isotherm model					
K_t (L/g)	8.62	7.66	2.60	5.04	2.50
b (J/mol)	392.9	320.9	335.7	88.73	138.4
R^2	0.87	0.93	0.99	0.98	0.85
Halsey isotherm model					
n_H	–1.12	–2.95	–3.22	–0.59	–1.33
K_H (mg/g)	2.99	0.0009	0.0003	0.15	1.90
R^2	0.93	0.93	0.97	0.86	0.90
Jovanovic isotherm model					
$q_{m,theo}$ (mg/g)	2.00	15.25	16.94	4.71	9.77
K_J	0.047	0.038	0.025	0.127	0.082
R^2	0.91	0.95	0.97	0.90	0.97
Elovich isotherm model					
$q_{m,theo}$ (mg/g)	163.9	11.3	12.8	12.9	23.7
K_E	3.62	19.29	28.91	32.18	34.3
R^2	0.50	0.96	0.97	0.85	0.91
Harkins–Jura isotherm model					
A (g/mg)	9.7	303	322	107	90
B (mg/g)	1.64	1.60	1.03	1.07	1.18
R^2	0.93	0.95	0.95	0.96	0.82

The Langmuir isotherm model explains the surface coverage by counterbalancing the relative rates of adsorption and desorption. The adsorption process depends on the open active sites of the adsorbent surface, while desorption depends on the covered adsorbent surface. Also, the Langmuir isotherm is used to demonstrate the relationship in monolayer coverage of the adsorbent. The model considers that the homogeneous active sites occur at the adsorbent surface and there are no interactions between two adsorbed molecules during the adsorption process. K_L is the Langmuir constant that presents the adsorption energy. Also, R_L indicates the adsorption to be unfavorable when R_L is over 1.0, favorable when R_L is in the range of 0.0 and 1.0, and irreversible when $R_L = 0$ [40]. The linear regression coefficient (R^2) values changed between 0.87 and 0.96, and the isotherm can be accepted fitting the Langmuir isotherm model well according to these results. K_L values were adjusted as 0.0062 L/mg for raw CS-PVA,

0.32 L/mg for AC/CS-PVA:3.0, and 0.054 L/mg for GO/CS-PVA:3.0, respectively. R_L values were calculated as 0.80, 0.15, 0.46, 0.50, and 0.32 for raw CS-PVA, raw AC, raw GO, AC/CS-PVA:3.0, and GO/CS-PVA:3.0, respectively (Fig. 8a). R_L values for all adsorbents were estimated between 0.0 and 1.0, and it can be concluded that ibuprofen adsorption was favorable. Despite the R^2, R_L and K_L values being suitable for fitting the model, $q_{m,\text{theo}}$ and $q_{m,\text{exp}}$ were estimated as 36.49 and 5.8; 45.45 and 11.5; 45.45 and 12.8; 52.35 and 10; and 17.0 and 66.67 mg/g for raw CS-PVA; raw AC; raw GO; AC/CS-PVA:3.0 and GO/CS-PVA:3.0, respectively (Table 5). Because of the differences between the experimental and theoretical q_e values, the Langmuir model did not fit the ibuprofen adsorption sufficiently.

The Freundlich isotherm is suitable for adsorption processes occurring on heterogeneous surfaces [41]. This model remarks the surface heterogeneity and the exponential distribution of active sites of the adsorbents [40]. K_F and $1/n$ indicate the relative adsorption capacity and the heterogeneity factor of the surface, respectively. The value of $1/n$ illustrates the adsorption to be favorable when $1/n$ is lower than 1.0, difficult when $1/n$ is between 0.5 and 1.0, and unfavorable when $1/n$ is over 1.0. The values of K_F and $1/n$ in the model were estimated as 25.70 mg/g and 3.72 for raw CS-PVA, and 2.09 mg/g and 1.69 for AC/CS-PVA:3.0, as indicated in Table 5. For the ibuprofen adsorption onto raw CS-PVA and AC/CS-PVA:3.0, $1/n$ values were higher than 1.0, so the Freundlich model is not favorable for the ibuprofen adsorption. Also, K_F and $1/n$ values were calculated as 4.07 and 0.75 for GO/CS-PVA:3.0, 15.84 mg/g and 0.362 for raw AC, and 6.60 mg/g and 0.557 for raw GO. The R^2 values of these adsorbents varied between 0.90 and 0.98, which are higher than those for the Langmuir isotherm (Fig. 8b, Table 5). It can be stated that for adsorbents having $1/n$ values lower than 1.0, the Freundlich model can be applied effectively for ibuprofen adsorption.

The Dubinin–Radushkevich (D–R) isotherm model expresses an adsorption mechanism with Gaussian energy distribution onto heterogeneous surfaces [42]. The model osculates the pore-filling mechanism [43]. The model assumes the multilayer character associated with Van der Waal's bonds and physical adsorption. Also, the characteristic factor of the D–R model is temperature dependent. Values of q_m and β (Table 5) were calculated as 45.60 and 1×10^{-6}, 36.96 and 3×10^{-6}, 45.60 and 8×10^{-5}, 62.80 and 2×10^{-5}, and 31.5 mg/g and 5×10^{-5} mol^{2}K/J^2 for raw CS-PVA, raw AC, raw GO, AC/CS-PVA:3.0, and GO/CS-PVA:3.0, respectively. The coefficient of determination calculated between 0.74 and 0.85 indicated a poor fit compared with the Freundlich model. 'Energy' is the Polanyi potential and mean free energy of adsorption, which are calculated using Table 4. An adsorption process is called physical if the value of 'Energy' is less than 8 kJ/mol, and it is called chemisorption if the 'Energy' values are between 8 and 16 kJ/mol [44]. The mean free energies were calculated between 79.05 and 707.10 J/mol (Fig. 8c, Table 5), which reflected the chemisorption of ibuprofen.

The Temkin isotherm model assumes that the heat of adsorption declines linearly while the adsorbent active sites are covered by adsorbent molecules, the adsorption is defined by a uniform distribution of binding energies of the adsorbent molecules, and the model approves the adsorbate–adsorbent interaction [45,46]. As shown in the equation in Table 4, K_T values were determined as 8.62, 7.66, 2.60, 5.04, and 2.50 L/g for raw CS-PVA, raw AC, raw GO, AC/CS-PVA:3.0, and GO/CS-PVA:3.0, respectively. Also, the heat of adsorption (b) values decreased from raw CS-PVA (392.9 J/mol) to GO/CS-PVA:3.0 (138.4 J/mol) biocomposites using ibuprofen adsorption. Based on the R^2 values (between 0.85 and 0.99) for all adsorbents, it is concluded that this model fits well to the equilibrium data.

The Halsey isotherm (Fig. 8e, Table 5) is suitable for multilayer adsorption onto a heterogeneous adsorbent surface [29]. The model fits the experimental data of ibuprofen adsorption well due to high correlation coefficient values, which can be an aspect of the heterogeneous distribution of active sites and multilayer adsorption on the raw materials and biocomposites [47]. Table 5 declares the better fitting to the adsorption data with regression coefficient in the range of 0.86 and 0.97 than the Langmuir isotherm; this result confirmed the heterogeneous surface of all the materials in the present study. Moreover, the Freundlich adsorption model results also confirmed the applicability of this model.

The Jovanovic model osculates on the theory of the Langmuir model, with the model assuming mechanical contact between the adsorbate and adsorbent. This is displayed in Fig. 8f and Table 5, for Jovanovic model's R^2 values were positioned within 0.91–0.97, which referred to an effective fit to the ibuprofen adsorption onto all materials. The Langmuir adsorption model's regression coefficient values being between 0.89 and 0.96 also confirmed the applicability of this model. Moreover, the openness of the $q_{m,\text{theo}}$ values (15.25, 16.9, and 9.77 mg/g for raw AC, raw GO, and AC/CS-PVA:3.0, respectively) and $q_{m,\text{exp}}$ results (11.5, 12.3, and 10.0 mg/g, respectively) did not suggest using this isotherm model and this model cannot be applied effectively for ibuprofen adsorption.

The Elovich isotherm model assumes that the active site of the adsorbent increases exponentially during the adsorption process and this implies a multilayer adsorption [38]. The Elovich maximum adsorption capacity and the Elovich constant can be calculated from the slope and intercept of the plot represented in Fig. 8, and model constants were calculated and are exhibited in Table 5. According to the results, $q_{m,\text{theo}}$ and $q_{m,\text{exp}}$ values were determined as 11.3 and 11.5, 12.8 and 12.3, 12.9 and 10.0, and 23.7 and 17.0 mg/g for raw AC, raw GO, AC/CS-PVA:3.0, and GO/CS-PVA:3.0, respectively. The results illustrate that the Elovich isotherm model can be applied to ibuprofen adsorption using these adsorbents. Also, the R^2 values of raw CS-PVA (0.50) and $q_{m,\text{theo}}$ (163.9 mg/g) and $q_{m,\text{exp}}$ (5.8 mg/g) values do not promote the model for using raw CS-PVA for ibuprofen adsorption (Fig. 8g, Table 5).

The Harkins–Jura isotherm model assumes multilayer adsorption occurring on an adsorbent surface having a heterogeneous pore distribution [48]. The values of constants A and B of the isotherm were calculated from plot $1/q_e^2$ vs. $\log C_e$ (Fig. 8h, Table 5). This model showed a better fit to the adsorption data than the Langmuir, D–R, and Halsey isotherm models, with R^2 values in the range of 0.82 and 0.96.

Based on the correlation coefficients (R^2), q_m values and other parameters of the models, the Freundlich, Temkin,

Halsey, Elovich, and Harkins–Jura isotherm models were fitted to the adsorption better than the Langmuir, D-R, and Jovanovic models. It can be concluded that the ibuprofen adsorption process occurred on the heterogeneous raw CS-PVA, AC, GO, and 3.0% (w/w) AC- and GO-embedded CS-PVA surfaces. Also, ibuprofen adsorption can be said to occur in a multilayer phase onto heterogeneous biocomposite surfaces. Active sites of the biocomposites increased logarithmically during the adsorption process because of the occurring multilayer adsorption and multilayer ibuprofen adsorption on the biocomposite surfaces having a heterogeneous pore distribution. Moreover, the heat of adsorption decreased linearly while the adsorbents' active sites were caked by ibuprofen molecules. The ibuprofen adsorption was characterized by a uniform bonding energy of the AC- and GO-embedded CS-PVA.

3.4. Adsorption kinetics

The effect of time on the adsorption of ibuprofen from wastewater is illustrated in Fig. 9. The ibuprofen adsorption onto raw CS-PVA was lower than for the other adsorbents during the 180 min. The adsorption kinetic curve for ibuprofen onto raw CS-PVA showed that the adsorption process reached equilibrium after 120 min and remained constant until the end of the experiment. Also, the adsorption processes with raw AC, raw GO, AC/CS-PVA:3.0, and GO/CS-PVA:3.0 reached equilibrium at the end of 100 min and C_e values were determined as nearly 5.8, 3.4, 9.5, and 3.5 mg/L, and q_e values were measured as 17.0, 18.3, 15.2, and 18.2 mg/g for raw AC, raw GO, AC/CS-PVA:3.0, and GO/CS-PVA:3.0, respectively, in this period. For AC/CS-PVA:3.0, nearly 76% of the ibuprofen was decontaminated after 100 min, while raw AC achieved this percentage within 50 min. Also, GO/CS-PVA:3.0 and raw GO presented the same recovery percentage after 100 min. It is clearly seen that the ibuprofen adsorption rate obtained by 3% (w/w) AC- and GO-embedded CS-PVA biocomposites make them effective as raw materials.

The kinetic studies were carried out with 100 mg of each adsorbent with 40 mg/L ibuprofen solution at 140 rpm during 180 min. The adsorption kinetics was described using the pseudo-first order, pseudo-second order [49], Weber–Morris [50], Elovich, and Bangham [27] models. The pseudo-first order model can be used for the adsorption of solid/liquid system, the pseudo-second order adsorption rate equation [51] considers the rate-determining step of the chemical reaction, and the Weber–Morris intraparticle diffusion model with a multilinearity correlation explains the mass transfer phenomena of the adsorption. The Elovich model explains heterogeneous systems for chemical sorption and the Bangham model assumes that pore diffusion controls the sorption rate [50]. The model equations are represented in Table 6.

The kinetic parameters of the models describing ibuprofen adsorption were estimated from the slope and intercept of the plots from the model equations (Table 7). The plots of $\ln(q_e-q_t)$ and t/q_t vs. time (min) were drawn (Figs. 10a and b), kinetics parameters were calculated from slope and intercept for pseudo-first order and pseudo-second order reaction kinetics, respectively, and rate constants k_1 (min^{-1}), k_2 (g/mg min) and initial adsorption rate h (mg/g min) were determined as constants of the models. Also, the plots of q_t against $t^{0.5}$ for the Weber–Morris intraparticle diffusion kinetic model are presented in Fig. 10c, and k_{id} (mg/g $min^{0.5}$) values were calculated as the rate constant. The plots of q_t vs. ln$t$ for Elovich's model are exhibited in Fig. 10d. According to the model, α (mg/g min) and β (g/mg) values represent the adsorption rate constant and the number of available sites for adsorption. The Bangham kinetic model is displayed in Fig. 10e. The calculated values of k_1, k_2, k_1d_1, k_1d_2, k_0, h, α, β, $q_{e,theo}$, and the R^2 values of ibuprofen adsorption onto the biocomposites are demonstrated in Table 7.

For the pseudo-first order model, although the experimental q_e values ($q_{e,exp}$) were found as 5.8, 11.5, 12.8, 10.0, and 17.0 mg/g for raw CS-PVA, raw AC, raw GO, AC/CS-PVA:3.0, and GO/CS-PVA:3.0, respectively. The q_e values were calculated from the model as 11.36, 17.6, 32.3, 15.1, and 26.2 mg/g for the same biocomposites, and the R^2 values changed between 0.95 and 0.99. According to the results, q_e values determined from the significantly different from experimental q_e values indicated the model is not suitable for describing the ibuprofen adsorption (Fig. 10a, Table 7).

For the pseudo-second order kinetic model, the R^2 values were estimated between 0.95 and 0.99 for all biocomposites,

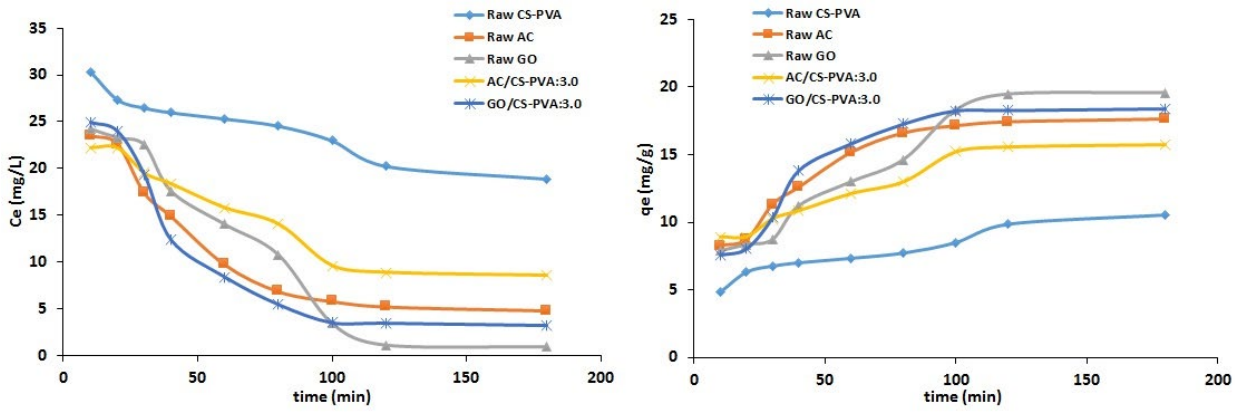

Fig. 9. Effect of time onto ibuprofen adsorption.

Table 6
Kinetic models equations

Pseudo-first order kinetic model	$\log\left(q_e - q_t\right) = \log q_e - \frac{k_1}{2.303}t$
Pseudo-second order kinetic model	$\frac{t}{q_t} = \frac{1}{k_2 q_e^2} + \frac{1}{q_e}t$
Weber–Morris intra-particle diffusion kinetic model	$q_t = k_{\mathrm{id}} t^{0.5} + C$
Elovich kinetic model	$q_t = \frac{1}{\beta}\ln\left(\alpha\beta\right) + \frac{1}{\beta}\ln t$
Bangham kinetic model	$\log\left[\log\left(\frac{C_0}{C_0 - q_t m}\right)\right] = \log\left(\frac{k_0 m}{2.303V}\right) + \alpha\log t$

Table 7
Kinetic model parameters of ibuprofen adsorption

	Raw CS-PVA	Raw AC	Raw GO	AC/CS-PVA:3.0	GO/CS-PVA:3.0
$q_{e,\mathrm{exp}}$ (mg/g)	5.8	11.5	12.8	10.0	17.0
Pseudo-first order kinetic model					
$q_{e,\mathrm{cal}}$ (mg/g)	11.36	17.6	32.3	15.1	26.2
k_1 (min^{-1})	0.015	0.035	0.037	0.032	0.045
R^2	0.82	0.98	0.78	0.86	0.95
Pseudo-second order kinetic model					
$q_{e,\mathrm{cal}}$ (mg/g)	6.6	9.9	16.4	13.5	21.5
k_2 (g/mg min)	3.7×10^{-3}	2.5×10^{-3}	1.0×10^{-3}	2.9×10^{-3}	1.9×10^{-3}
h (mg/g min)	0.16	0.24	0.27	0.53	0.87
R^2	0.97	0.99	0.95	0.98	0.98
Weber–Morris intra-particle diffusion kinetic model					
k_{id1} (mg/g $\mathrm{min}^{0.5}$)	0.68	1.45	0.94	0.66	1.93
R^2	0.91	0.90	0.87	0.84	0.84
k_{id2} (mg/g $\mathrm{min}^{0.5}$)	0.53	0.13	0.31	0.13	0.04
R^2	0.81	0.89	0.77	0.80	0.98
Elovich kinetic model					
β (g/mg)	0.54	0.25	0.20	0.35	0.21
α (mg/g min)	2.30	5.99	15.6	4.06	11.2
R^2	0.91	0.94	0.89	0.91	0.93
Bangham kinetic model					
k_0 (L/g)	1.86	1.34	1.86	1.12	1.69
α	0.25	0.31	0.38	0.23	0.37
R^2	0.94	0.94	0.92	0.93	0.92

and the experimental q_e values were nearly the same as the calculated ones (for raw CS-PVA $q_{e,\mathrm{exp}}$ = 5.8 mg/g and $q_{e,\mathrm{cal}}$ = 6.6 mg/g; for raw AC $q_{e,\mathrm{exp}}$ = 11.5 mg/g and $q_{e,\mathrm{cal}}$ = 9.9 mg/g; for raw GO $q_{e,\mathrm{exp}}$ = 12.8 mg/g and $q_{e,\mathrm{cal}}$ = 16.4 mg/g; and for GO/CS-PVA:3.0 $q_{e,\mathrm{exp}}$ = 17.0 mg/g and $q_{e,\mathrm{cal}}$ = 21.5 mg/g). The adsorption rate constants, h, were calculated as 0.16, 0.24, 0.27, 0.53, and 0.87 mg/g min for raw CS-PVA, raw AC, raw GO, AC/CS-PVA:3.0, and GO/CS-PVA:3.0, respectively (Fig. 10b, Table 7). These results implied that, the ibuprofen adsorption onto all biocomposites was represented better by the pseudo-second order kinetic model than the other.

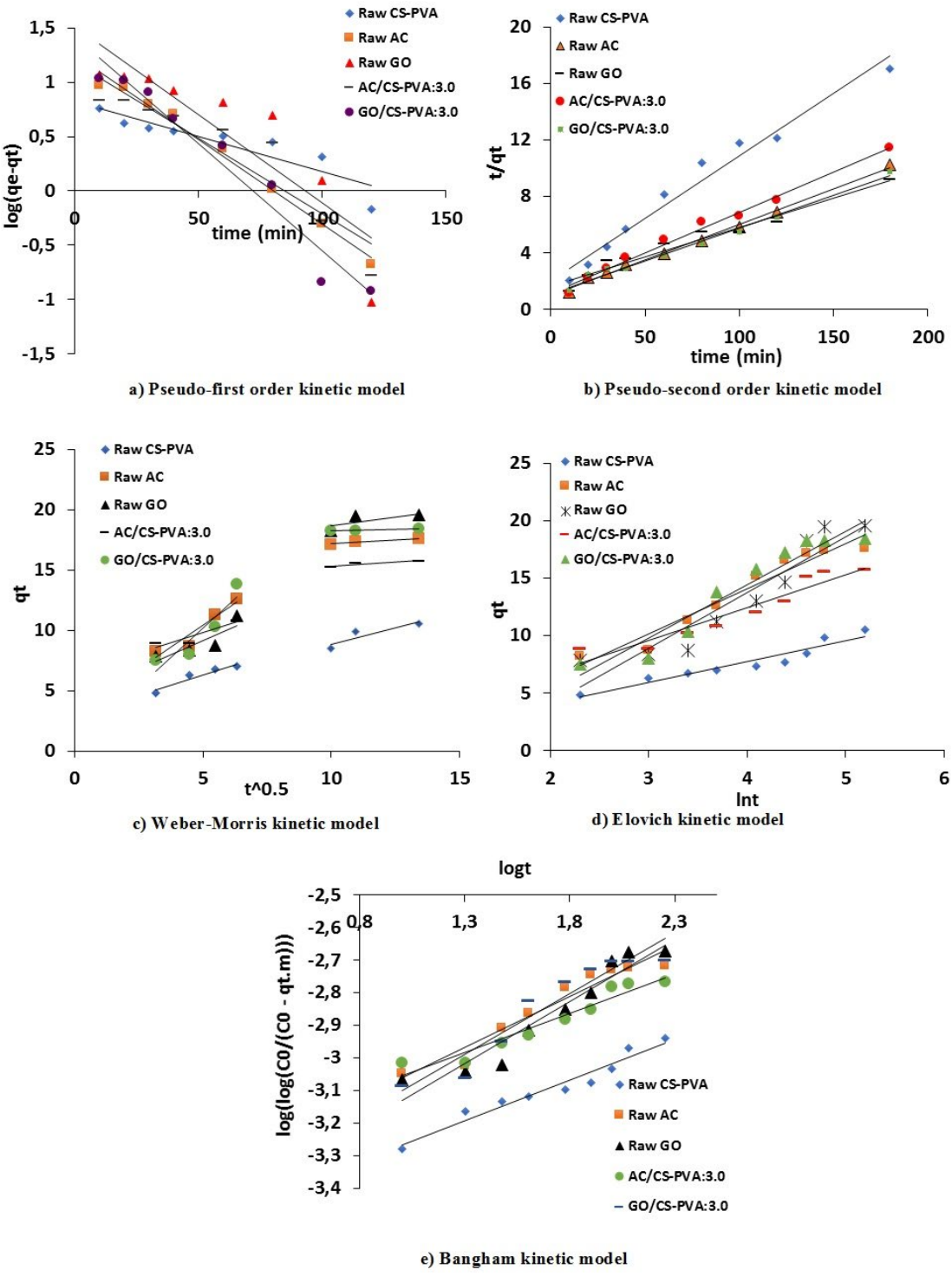

Fig. 10. Kinetic study of ibuprofen adsorption.

The R^2 values for Weber–Morris intraparticle diffusion were calculated between 0.84 and 0.91, which was lower than the pseudo-second order kinetic model. From Fig. 10c and Table 7, two separate multilinear phases were indicated, which can be explained as different mass transfer phenomena occurring. The first sharper linear part (phase I, first 40 min) showed the boundary layer diffusion effect and mass transfer through the external surface of biocomposites. The second linear part (phase II) characterized the intraparticle diffusion effect and gradual mass transfer. According to Table 7, k_{id1} and k_{id2} for all biocomposites demonstrated that intraparticle diffusion rates were slower than the boundary layer mass

transfer rate. Also, k_{id1} and k_{id2} constants for AC/CS-PVA:3.0 and GO/CS-PVA:3.0 were calculated as k_{id1} = 0.66 mg/g min$^{0.5}$ and k_{id2} = 0.13 mg/g min$^{0.5}$ and also k_{id1} = 1.93 mg/g min$^{0.5}$ and k_{id2} = 0.04 mg/g min$^{0.5}$, respectively. These results described the boundary layer mass transfer rate as fivefold and fifty-fold the interior mass transfer for AC/CS-PVA:3.0 and GO/CS-PVA:3.0 biocomposites, respectively.

The correlation coefficients (R^2) for the Elovich model were determined to be 0.89–0.94 and the initial adsorption rate (α) values of all the biocomposites increased significantly with embedding activated carbon and graphene oxide into the CS-PVA ($\alpha_{AC/CS\text{-}PVA:3.0}$ = 4.06 mg/g min and $\alpha_{GO/CS\text{-}PVA:3.0}$ = 11.2 mg/g min). It can be safely stated that Elovich's model fits sufficiently the ibuprofen adsorption (Fig. 10d).

The R^2 values were determined to be between 0.92 and 0.94 for the Bangham model, so pore diffusion played an important role during the ibuprofen adsorption.

3.5. Thermodynamics

The standard thermodynamic parameters during the adsorption process were evaluated and are presented in Table 8. The adsorption of ibuprofen by AC/CS-PVA.3.0 and GO/CS-PVA:3.0 was spontaneous with the negative values of ΔG^o [27,28]. The negative Gibbs free energy showed that adsorption was a spontaneous process and decreased with increasing temperature, which indicates the spontaneous behavior of ibuprofen adsorption onto biocomposites changed inversely with temperature.

For all temperatures and both biocomposites, negative Gibbs free energy values pointed out that AC- and GO-embedded CS-PVA biocomposites spontaneously adsorbed ibuprofen. $\Delta S°$ values were determined as 176.5 kJ/mol and 241.3 J/mol K for AC/CS-PVA:3.0 and GO/CS-PVA:3.0, respectively. The positive $\Delta S°$ values indicated an increasing disorderliness and chaos at the biocomposite/ibuprofen interface and the affinity of biocomposites toward ibuprofen. $\Delta H°$ values of ibuprofen adsorption were calculated as 51.6 and 67.3 kJ/mol using AC/CS-PVA:3.0 and GO/CS-PVA:3.0, respectively. This described that the ibuprofen adsorption onto these biocomposites was endothermic in nature. The endothermic behavior of ibuprofen adsorption was proved by the positive values of enthalpy and also the positive/negative values can be used to identify chemical or physical adsorption. For chemical adsorption, $\Delta H°$ is higher than 35 kJ/mol, while for physical adsorption it is lower than 35 kJ/mol. As can be seen clearly from Table 8, the positive $\Delta H°$ values indicated ibuprofen adsorption for AC- and GO-embedded CS-PVA were an endothermic reaction, so an increase of temperature promotes the adsorption reaction. As a result, it can be concluded that ibuprofen adsorption using AC/CS-PVA:3.0 and GO/CS-PVA:3.0 as adsorbents is a chemical adsorption process.

3.6. Modeling of the adsorption process using the central composite design

According to the CCD experimental design matrix, the adequacy of models that were evaluated (linear, two factors interactive [2FI], quadratic, and cubic models) was described in Table 9. Linear, interactive (2FI), quadratic, and cubic models were adapted to the experimental studies to obtain

Table 8
Thermodynamic parameters of ibuprofen adsorption

Biocomposite	$\Delta H°$ (kJ/mol)	$\Delta S°$ (J/molK)	$\Delta G°$ (kJ/mol)			
			303 K	313 K	323 K	333 K
AC/CS-PVA:3.0	51.6	176.5	–1.8	–3.6	–5.4	–7.1
GO/CS-PVA:3.0	67.3	241.3	–5.8	–8.2	–10.6	–13.0

Table 9
Regression statics models of ibuprofen adsorption

Source	Standard Deviation	R^2	R^2_{adj}	R^2_{pre}	Press	
AC/CS-PVA:3.0						
Linear	10.25	0.74	0.69	0.63	3,716.09	
Interactive (2FI)	10.26	0.80	0.69	0.37	6,307.13	
Quadratic	*8.05*	*0.90*	*0.81*	*0.44*	*5,599.20*	*Suggested*
Cubic	9.98	0.93	0.71	–9.10	100,476.00	Aliased
GO/CS-PVA:3.0						
Linear	7.41	0.80	0.77	0.71	2,016.56	
Interactive (2FI)	7.98	0.82	0.73	0.64	2,481.48	
Quadratic	*3.42*	*0.97*	*0.95*	*0.85*	*1,010.40*	*Suggested*
Cubic	2.94	0.99	0.96	–0.26	8,724.00	Aliased

the regression statistics models. The adequacy of the models was decided by two different tests, which are sequential model sum of squares and model summary statistics tests [51,52].

In the present study, the fit summary of the data displays that the quadratic model was statistically extremely significant, the p value of the model was lower than 0.0001, and also the standard deviation and regression coefficient of the model were acceptable for ibuprofen adsorption using both biocomposites. These results also pointed out that the quadratic model was statistically powerful for adsorption of ibuprofen and the quadratic model is suggested to describe the relationship between responses and independent process variables. From Table 9, it was found that the quadratic model has a relatively high R^2_{adj} and a smaller standard deviation than in the other models. R^2 and standard deviation values were determined to be 0.90 and 8.05 using AC/CS-PVA:3.0 and 0.97 and 3.4 using GO/CS-PVA:3.0. It can be stated that the terms in the regression quadratic model have a significant correlation with ibuprofen removal percentage. The cubic model was found to be aliased. Although R^2_{adj} and R^2 values were higher than in the quadratic model, the standard deviation and R^2_{pre} values were not suitable for selecting this model. Hence, the quadratic model was selected as the suitable model for further analysis.

The statistical significance of the regression equation was checked by ANOVA analysis and Fisher's F-test value (F-value) for the response surface quadratic polynomial model, which is shown in Table 10.

An empirical relationship between the responses and the four independent variables has been expressed in quadratic model equations in terms of actual variables in Eq. (4) for AC/CS-PVA:3.0 and Eq. (5) for GO/CS-PVA:3.0:

$$\text{Removal}\%\left(\frac{\text{AC}}{\text{CS}}-\text{PV A}\right)=-7.66406-1.18229A+3.25729B+0.79427C-0.11510D+3.125\times10^{-3}AB-1.5625\times10^{-3}AC+0.15156AD+5.9375\times10^{-3}BC-2.18750\times10^{-3}BD+2.34375\times10^{-3}CD-1.10156A^2-0.035312B^2-7.26562\times10^{-3}C^2-8.82813\times10^{-3}D^2 \quad (4)$$

$$\text{Removal}\%\left(\frac{\text{GO}}{\text{CS}}-\text{PVA}\right)=-80.26302+21.07812A+1.75729B+0.90260C+0.89115D-0.020312AB-0.020312AC-0.060937AD-2.81250\times10^{-3}BC-3.43750\times10^{-3}BD-3.90625\times10^{-3}CD-1.53385A^2-6.35417B^2-1.58854\times10^{-3}C^2-1.90104\times10^{-3}D^2 \quad (5)$$

where A, B, C, and D are expressed as a pH, temperature (°C), amount of biocomposite (mg) and ibuprofen concentration (mg/L), respectively, for quadratic model equations (Table 10). The equation terms, such as AB, AC, BC, BD, and CD, symbolize the interaction of two independent variables, A^2, B^2, C^2, and D^2 symbolize the squared effect of independent variables. The negative and positive signs of parameter coefficients show decrease and increase in the responses, with an increase in the independent process variables. Eqs. (4) and (5) indicate not only the independent variables but also the interactions and squared effects of independent variables, which were very important for removal of ibuprofen by using AC- and GO-embedded CS-PVA as adsorbents.

Experimental data were examined using ANOVA analysis, and the analysis was used to control the statistical significance of the quadratic model by checking the p-value (probability value) and the F-value. In the ANOVA analysis, a model with a high F-value and a low p-value (less than 0.05) is considered to be suitable [52]. The outputs of the ANOVA of the quadratic model and the F-values for the removal of ibuprofen using AC/CS-PVA:3.0 and GO/CS-PVA:3.0 are given in Table 10. As can be seen from the table, it was found that the p-values of both models were smaller than 0.0001. Moreover, the F-values were determined as 9.9 for the model of AC/CS-PVA:3.0 and 41.1 for GO/CS-PVA:3.0. The very low p-values and relatively high F-values in both models indicated that the quadratic models were significant and suggest a good relation between response and independent variables for the ibuprofen adsorption using AC- and GO-embedded CS-PVA. On the other hand, the lowest calculated p-value or the highest calculated F-value of model variables showed the most effective variables on the response. According to p-values, A, B, C, AD, A^2, B^2, and D^2 for AC/CS-PVA:3.0 and A, B, C, D, AD, and A^2 for GO/CS-PVA:3.0 were extremely significant model variables. Furthermore, according to the F-values, the most effective model variables for AC/CS-PVA:3.0 and GO/CS-PVA:3.0 were observed as A (pH) with 82.9 and 310.1, respectively. Besides, the most effective variables on the response were, in order, $B > C > AD > A^2 > B^2 = D^2$ using AC/CS-PVA:3.0 and $B > A^2 > C > D > AD$ using GO/CS-PVA:3.0 as adsorbents for ibuprofen adsorption.

3.7. Response surface analysis

Three-dimensional (3D) response surface plots are very useful to explain the interaction effects of the variables on the responses. Also, 3D-response surface graphs (Figs. 11a–f and Figs. 12a–f) for ibuprofen adsorption percentage were obtained based on the quadratic polynomial model (Eqs. (4) and (5)). Since the regression model has four independent variables and two factors remained constant at the center levels, so six response 3D surfaces were obtained. The 3D-response surfaces presented the reasonable interactions between each of the independent factors and the ibuprofen removal percentage.

In the present study, the effects of independent parameters on ibuprofen adsorption were examined. 3D-response surface plots were drawn based on the quadratic model established Eqs. (4) and (5) and illustrated in Figs. 11 and 12 for AC/CS-PVA:3.0 and GO/CS-PVA:3.0 biocomposites, respectively.

Figs. 11a–c and Figs. 12a–c indicate the effects of pH on ibuprofen removal percentage while keeping the other two factors at the center level. Increasing pH values displayed a negative effect on the adsorption of ibuprofen using both adsorbents. As the pH of the solution ranged from the acidic region to the basic, the adsorption of ibuprofen was negatively affected due to the electrostatic repulsive forces between the ibuprofen molecules and the surface of the

Table 10
ANOVA analysis and *F*-test data of ibuprofen adsorption

Source	Sum of squares	*df*	Mean square	*F*-value	*p*-value prob > *F*	
AC/CS-PVA:3.0						
Model	8,973.4	14	641.0	9.9	<0.0001	Significant
A	5,370.0	1	5,370.0	82.9	<0.0001	
B	1,107.0	1	1,107.0	17.1	0.0009	
C	805.0	1	805.0	12.4	0.0031	
D	35.0	1	35.0	0.5	0.47	
AB	0.063	1	0.063	0.00096	0.98	
AC	0.063	1	0.063	0.00096	0.98	
AD	588.1	1	588.1	9.07	0.01	
BC	22.6	1	22.6	0.35	0.56	
BD	3.1	1	3.1	0.05	0.83	
CD	14.1	1	14.1	0.22	0.65	
A^2	532.5	1	532.5	8.22	0.01	
B^2	342.0	1	342.0	5.2	0.04	
C^2	231.7	1	231.7	3.5	0.08	
D^2	342.0	1	342.0	5.2	0.04	
Residual	972.1	15	64.8			
GO/CS-PVA:3.0						
Model	6,722.1	14	480.1	41.1	<0.0001	Significant
A	3,626.0	1	3,626.0	310.1	<0.0001	
B	1,247.0	1	1,247.0	106.6	<0.0001	
C	477.0	1	477.0	40.8	<0.0001	
D	176.0	1	176.0	15.1	0.0015	
AB	3.1	1	3.1	0.3	0.62	
AC	10.6	1	10.6	0.9	0.36	
AD	95.1	1	95.1	8.1	0.01	
BC	5.06	1	5.1	0.4	0.52	
BD	7.56	1	7.6	0.6	0.43	
CD	39.1	1	39.1	3.3	0.09	
A^2	1,032.5	1	1,032.5	88.3	<0.0001	
B^2	11.1	1	11.1	0.9	0.35	
C^2	11.1	1	11.1	0.9	0.35	
D^2	15.9	1	15.9	1.4	0.26	
Residual	175.4	15	11.7			

biocomposites. It can be followed from Figs. 11a and 12a that the ibuprofen adsorption percentage was higher at acidic and neutral pHs than at basic pH values. The maximum removal percentages were found at pH 3.0 and 5.0 and ibuprofen removal percentage values were determined as 82% at pH 3.0 and 83% at pH 5.0 using AC/CS-PVA:3.0 (Fig. 11a). Also, the removal percentage values were found at pH 7.0 with 94% and pH 5.0 with 93% for GO/CS-PVA:3.0 (Fig. 12a). At lower pHs, the positive charge on the surface of the biocomposite increased because of the PZC of the biocomposites and that enabled it to adsorb ibuprofen with interaction between the molecules. Additionally, the surface charges of the biocomposites were negative in the basic pH region, the electrostatic repulsion force occurred, and adsorption efficiency decreased sharply. Similar results were also reported in the literature for different adsorbent systems.

The combined effects of temperature with pH, the amount of biocomposite, and the ibuprofen concentration are shown in Figs. 11a, d, e and Figs. 12a, d, e, respectively. The temperature displayed a positive quadratic effect on the ibuprofen removal percentage (Table 10). It was clearly seen from Fig. 11a that the temperature showed a positive effect between 20°C and 50°C and also indicated a negative effect above 50°C for the removal percentage of ibuprofen using AC/CS-PVA:3.0 as an adsorbent. The maximum and minimum removal percentages of ibuprofen were determined as 83% and 15% at 50°C and 20°C, respectively. Besides, the ibuprofen removal percentage showed the same trend (Fig. 12a) between 20°C and 60°C, with the maximum removal percentage being found at 60°C with a 94% removal percentage using GO/CS-PVA:3.0. As the temperature increased in the range between 20°C and 60°C, the ibuprofen removal

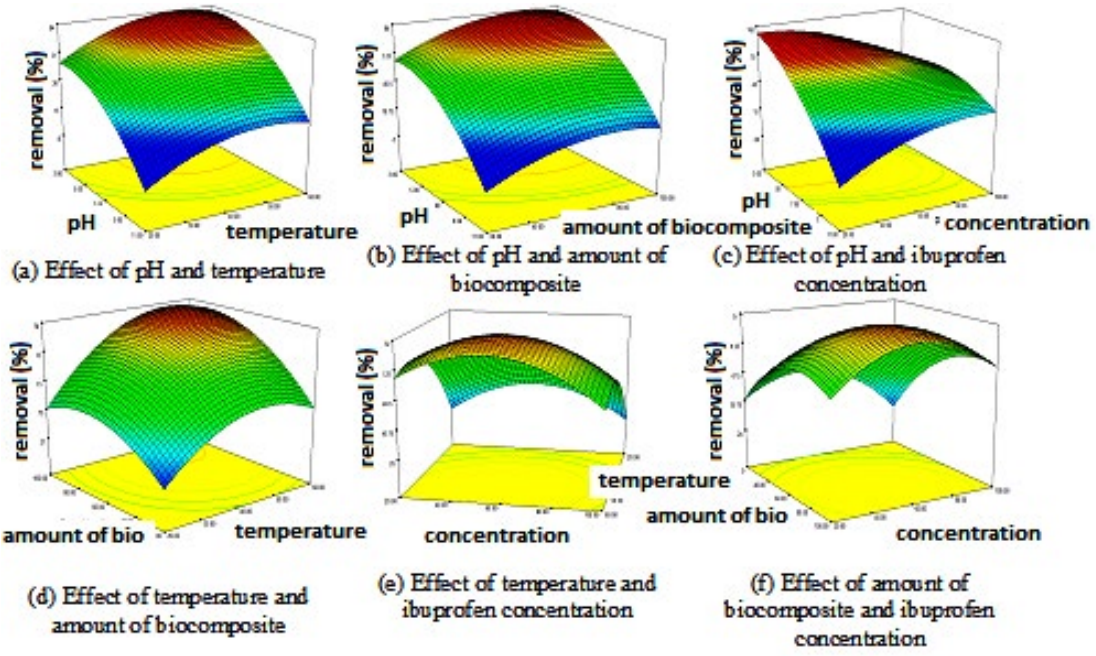

Fig. 11. Effect of process variables on ibuprofen adsorption using AC/CS-PVA.

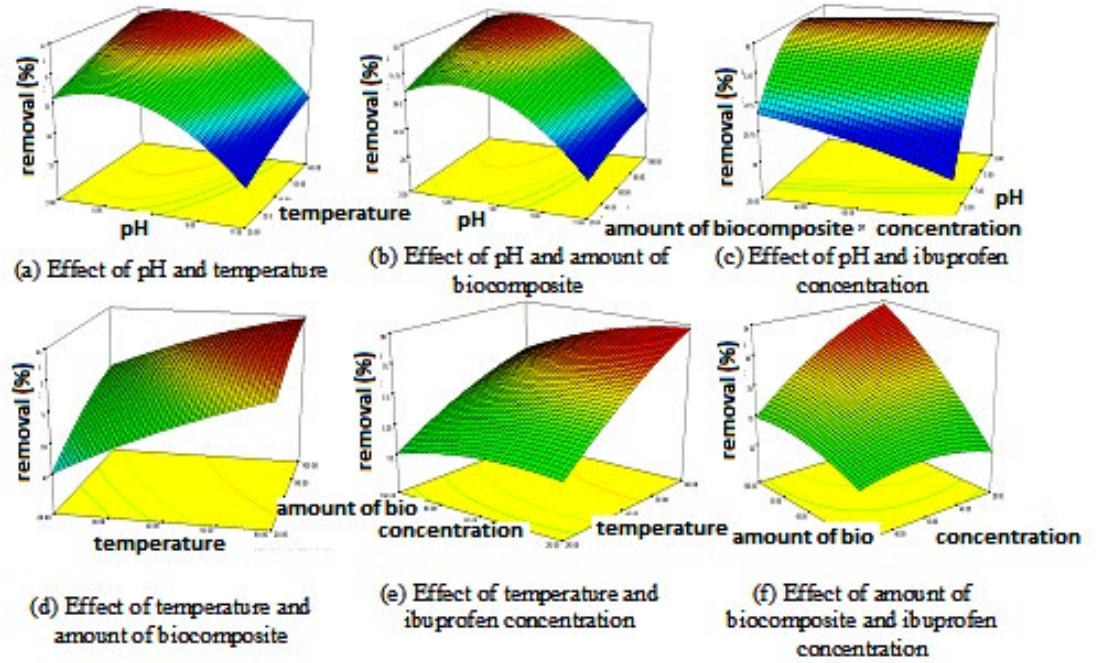

Fig. 12. Effect of process variables on ibuprofen adsorption using GO/CS-PVA.

percentage increased effectively, demonstrating that ibuprofen adsorption was encouraged at rising temperatures. This can be explained by the incremental increase of the kinetic energy of the ibuprofen molecules.

The combined effects of the amount of biocomposite corresponding with pH, temperature, and ibuprofen concentration are presented in Figs. 11b, d, f and Figs. 12b, d, f, respectively. From the figures, biocomposite amount had a positive effect on the removal percentages for ibuprofen adsorption while the dosage of the adsorbent increased from a low to a high level. An incremental increase in the amount of AC- and GO-embedded CS-PVA biocomposites enhanced the surface area and pore volume of the adsorbent as well as the accessibility of active sites to ibuprofen; hence the ibuprofen removal percentage was boosted effectively.

Table 11
Model confirmation

	pH	Temperature (°C)	Amount of biocomposite (mg)	Ibuprofen concentration (mg)	Removal (%) (experimental)	Removal (%) (predicted)
AC/CS-PVA:3.0	5.0	50	80	40	83	82.5
GO/CS-PVA:3.0	5.0	50	80	40	93	97.9

Table 12
Comparison of the AC- and GO-embedded CS-PVA with other adsorbents

Pharmaceutical compounds	Biocomposite	Removal %	Reference
Bisphenol-A	Carbon fiber/chitosan–PVA	98%	[25]
Naproxen	Activated carbon/chitosan–PVA	97%	[27]
Ibuprofen	Fruit shell	87%	[31]
Ciprofloxacin	Composite	88%	[34]
Ibuprofen	Clay	84%	[39]
Naproxen	Clay	84%	[39]
Carbamazepine	Clay	88%	[39]
Ibuprofen	Activated carbon	94%	[51]
Ibuprofen	Activated carbon/chitosan–PVA	83%	This work
Ibuprofen	Grapheneoxide/chitosan–PVA	94%	This work

The interaction between ibuprofen concentration, pH, temperature, and amount of biocomposite is given in Figs. 11c, e, f and Figs. 12c, e, f. The removal percentage of ibuprofen increased as the initial ibuprofen concentration increased from 20 to 60 mg/L using AC/CS-PVA:3.0 and from 20 to 40 mg/L using GO/CS-PVA:3.0. It decreased sharply above 40 and 60 mg/L using AC/CS-PVA:3.0 and GO/CS-PVA:3.0, respectively. This can be explained by the ibuprofen molecules reaching the active sites on the biocomposite surfaces with low ibuprofen solution concentration. After 40 and 60 mg/L, the active sites are filled with ibuprofen molecules and the removal percentages decreased sharply. The percentage of ibuprofen removal declined with an increase in ibuprofen concentration at a high level and the unavailability of active sites for ibuprofen molecules on biocomposites due to higher concentrations can be the reason for this situation.

3.8. Process optimization

The batch ibuprofen adsorption experiments at the optimal conditions were further conducted to justify the suitability of the introduced model. According to the results indicated in Table 11, the experimental results for ibuprofen removal percentage were attained at 83% and 93% which is close to the predicted values of 82.5% and 97.9% for AC/CS-PVA:3.0 and GO/CS-PVA:3.0, respectively. This illustrated the high compatibility of the model with the experimental data.

Comparison of the maximum pharmaceutical compounds removal % values of different adsorbents with that of previously reported adsorbents/composites is investigated and the results are represented in Table 12. The table shows that AC- and GO-embedded CS-PVA can be used effectively for the removal of ibuprofen from wastewater.

4. Conclusion

In the present study, AC- and GO-embedded CS-PVA biocomposites were synthesized and applied for adsorption of ibuprofen, a nonsteroidal anti-inflammatory drug. Ibuprofen removal performances increased from nearly 83% to 94% by increasing AC and GO content. Adsorption isotherms have been expressed by the models of Langmuir, Freundlich, Dubinin–Radushkevich (D–R), Temkin, Halsey, Jovanovic, Elovich, Harkins–Jura, and Freundlich. It was found that the isotherm models of Temkin, Halsey, Elovich, and Harkins–Jura were fitted to ibuprofen adsorption. Also, adsorption kinetics was investigated and ibuprofen adsorption onto the biocomposites represented by the pseudo-second order, Bangham, and Elovich kinetic models. By evaluating the data of adsorption isotherms, kinetic and thermodynamic parameters, and optimization data, it can be safely concluded that AC- and GO-embedded CS-PVA biocomposites have the potential to be the most efficient adsorbents for the adsorption of pharmaceutical pollutants from wastewater.

References

[1] C.G. Daughton, A. Ternes, Thomas, Pharmaceuticals and personal care products in the environment: agents of subtle change, Environ. Toxicol., 28 (2009) 2663–2670.
[2] W. Zhang, K. Blum, M. Gros, L. Ahrens, H. Jernstedt, K. Wiberg, P.L. Andersson, B. Björlenius, G. Renman, Removal of micropollutants and nutrients in household wastewater using organic and inorganic sorbents, Desal. Wat. Treat., 120 (2018) 88–108.
[3] A.B.A. Boxall, M.A. Rudd, B.W. Brooks, D.J. Caldwell, K. Choi, S. Hickmann, E. Innes, K. Ostapyk, J.P. Staveley, T. Verslycke, G.T. Ankley, K.F. Beazley, Pharmaceuticals and personal care products in the environment: what are the big questions, Environ. Health Perspect., 120 (2012) 1221–1230.

[4] U. Taro, T. Kikuta, Separate estimation of adsorption and degradation of pharmaceutical substances and estrogens in the activated sludge process, Water Res., 39 (2005) 1289–1300.
[5] O.A. Jones, J.N. Lester, N. Voulvoulis, Pharmaceuticals: a threat to drinking water, Trends Biotechnol., 23 (2005) 163–167.
[6] G.Z. Kyzas, J. Fu, N.K. Lazaridis, D.N. Bikiaris, K.A. Matis, New approaches on the removal of pharmaceuticals from wastewaters with adsorbent materials, J. Mol. Liq., 209 (2015) 87–93.
[7] A. Vogt, P.A. Mcpherson, X. Shen, G. Zhu, S. Brianne, S.G. Nelson, M. Tsang, B.W. Day, High-content analysis of cancer-cell-specific apoptosis and inhibition of in vivo angiogenesis by synthetic (-)-pironetin and analogs, Chem. Biol. Drug Des., 74 (2009) 358–368.
[8] M. Gros, M. Petrovi, A. Ginebreda, D. Barceló, Removal of pharmaceuticals during wastewater treatment and environmental risk assessment using hazard indexes, Environ. Int., 36 (2010) 15–26.
[9] S.R. Khudhaier, A.A. Awad, D.T.A. Al-Heetimi, A.J.M. Al-Karawi, E.M. Al-Kinani, A.B. Omar Ali, Z.H.J. Al-Qaisi, Q.Z. Khalaf, Synthesis of chitosan–iron keplerate composite as an adsorbent for removal of toxic ions from water, Desal. Wat. Treat., 157 (2019) 165–176.
[10] B. Kasprzyk-hordern, R.M. Dinsdale, A.J. Guwy, The occurrence of pharmaceuticals, personal care products, endocrine disruptors and illicit drugs in surface water in South Wales, UK, Water Res., 42 (2008) 3498–3518.
[11] D. Kolpin, E. Furlong, S. Zaugg, Pharmaceuticals, hormones, and other organic wastewater contaminants in U.S. streams, 1999–2000: a national reconnaissance, Environ. Sci. Technol., 36 (2002) 1202–1211.
[12] R.H. Lindberg, B.A. V Andersson, Screening of human antibiotic substances and determination of weekly mass flows in five sewage treatment plants in Sweden, Environ. Sci. Technol., 39 (2005) 3421–3429.
[13] E.W.P. Westerhoff, Y. Yoon, S. Snyder, Fate of endocrine-disruptor, pharmaceutical, and personal care product chemicals during simulated drinking water treatment processes, Environ. Sci. Technol., 39 (2005) 6649–6663.
[14] I.M. Sebastine, R.J. Wakeman, Consumption and environmentel hazards of pharmaceutical substances ın the UK, Process Saf. Environ., 81 (2003) 229–235.
[15] N.S. Williams, M.B. Ray, H.G. Gomaa, Removal of ibuprofen and 4-isobutylacetophenone by non-dispersive solvent extraction using a hollow fibre membrane contactor, Sep. Purif. Technol., 88 (2012) 61–69.
[16] T.A. Ternes, Occurrence of drugs in German sewage treatment plants and rivers, Water Res., 32 (1998) 3245–3260.
[17] G.K. Ramesh, A. Vijaya Kumar, H.B. Muralidhar, S. Sampath, Graphene and graphene oxide as effective adsorbents toward anionic and cationic dyes, J. Colloid Interface Sci., 361 (2011) 270–277.
[18] H. Yamamoto, Y. Nakamura, S. Moriguchi, Y. Nakamura, Y. Honda, I. Tamura, Y. Hirata, A. Hayashi, J. Sekizawa, Persistence and partitioning of eight selected pharmaceuticals in the aquatic environment: laboratory photolysis, biodegradation, and sorption experiments, Water Res., 43 (2009) 351–362.
[19] S. Kyu, S.K. Sharma, C.D.T. Abel, A. Magic-knezev, G.L. Amy, Role of biodegradation in the removal of pharmaceutically active compounds with different bulk organic matter characteristics through managed aquifer recharge: batch and column studies, Water Res., 45 (2011) 4722–4736.
[20] M.B. Ahmed, J.L. Zhou, H.H. Ngo, W. Guo, Adsorptive removal of antibiotics from water and wastewater: progress and challenges, Sci. Total Environ., 532 (2015) 112–126.
[21] J. Torres-Pérez, C. Gérente, Y. Andrès, Sustainable activated carbons from agricultural residues dedicated to antibiotic removal by adsorption, Chin. J. Chem. Eng., 20 (2012) 524–529.
[22] D. Chen, H. Feng, J. Li, Graphene oxide: Preparation, functionalization and electrochemical applications, Chem. Rev., 112 (2012) 6027–6053.
[23] B.F. Machado, P. Serp, Graphene-based materials for catalysis, Catal. Sci. Technol., 2 (2012) 54–75.
[24] H. Mittal, S.S. Ray, B.S. Kaith, J.K. Bhatia, J. Sharma, S.M. Alhassan, Recent progress in the structural modification of chitosan for applications in diversified biomedical fields, Eur. Polym. J., 109 (2018) 402–434.
[25] E.B. Simsek, D. Saloglu, N. Ozcan, I. Novak, D. Berek, Carbon fiber embedded chitosan/pva composites for decontamination of endocrine disruptor bisphenol-a from water, J. Taiwan Inst. Chem. Eng., 70 (2017) 291–301.
[26] S. Sunaric, M. Petkovic, M. Denic, S. Mitic, Determination of ibuprofen in combined dosage forms and cream by direct UV spectrophotometry after solid-phase extraction, Acta Pol. Pharm. Res., 70 (2013) 403–411.
[27] D. Saloglu, N. Ozcan, Activated carbon embedded chitosan/polyvinyl alcohol biocomposites for adsorption of nonsteroidal anti-inflammatory drug-naproxen from wastewater, Desal. Wat. Treat., 107 (2018) 72–84.
[28] A. Abishkek, N. Saranya, P. Chandi, N. Selvaraju, Studies on the remediation of chromium(IV) from simulated wastewater using novel biomass of *Pinus kesia* cone, Desal. Wat. Treat., 114 (2018) 192–204.
[29] N. Saranya, A. Ajmani, V. Sivasubramanian, N. Selvaraju, Hexavalent chromium removal from simulated and real effluent using *Artocarpus heterophyllus* peel biosorbent- Batch and continuous studies, J. Mol. Liq., 265 (2018) 779–790.
[30] R. Farouq, N.S. Yousef, Equilibrium and kinetics studies of adsorption of copper (II) ions on natural biosorbent, Int. J. Chem. Eng. Appl., 6 (2015) 319–324.
[31] N. Sivarajasekar, N.M. Raj, K. Balasubramani, G. Moorthy, I. Muthu, Optimization, equilibrium and kinetic studies on ibuprofen removal onto microwave assisted-activated *Aegle marmelos correa* fruit shell, Desal. Wat. Treat., 84 (2017) 48–58.
[32] M. Mushtaq, T. Isa, L. Ismail, M. Nadeem, M. Sagir, R. Azam, R. Hashmet, Influence of PZC (Point of zero charge) on the static adsorption of anionic surfactants on a Malaysian sandstone, J. Dispers. Sci. Technol., 35 (2014) 343–349.
[33] U. Domañska, A. Pobudkowska, A. Pelczarska, P. Gierycz, pKa and solubility of drugs in water, ethanol, and 1-octanol, J. Phys. Chem. B, 113 (2009) 8941–8947.
[34] Y. Wu, Y. Tang, L. Li, P. Liu, X. Li, W. Chen, Y. Xue, The correlation of adsorption behavior between ciprofloxacin hydrochloride and the active sites of Fe-doped MCM-41, Front. Chem., 6 (2018) 1–11.
[35] E. Nakkeeran, N. Saranya, M.S. Giri Nandagapol, A. Santhiagu, N. Selvaraju, Hexavalent chromium removal from aqueous solutions by a novel powder prepared from *Colocasia esculenta* leaves, Int. J. Phytorem., 18 (2016) 812–821.
[36] A. Gunay, E. Arslankaya, I. Tosun, Lead removal from aqueous solution by natural and pretreated clinoptilolite: adsorption equilibrium and kinetics, J. Hazard. Mater., 146 (2007) 362–371.
[37] M.R. Samarghandi, M. Hadi, S. Moayedi, F.B. Askari, Two-parameter isotherms of methyl orange sorption by pinecone derived activated carbon, Iranian J. Environ. Health Sci. Eng., 6 (2009) 285–294.
[38] M. Gubernak, W. Zapala, K. Tyrpien, K. Kaczmarski, Analysis of amylbenzene adsorption equilibria on different RP-HPLC, ACTA Chromatogr., 13 (2003) 38–59.
[39] H. Khazri, I. Ghorbel-Abid, R. Kalfat, M. Ayadi, Removal of ibuprofen, naproxen and carbamazapine in aqueous solution onto natural clay: equilibrium, kinetics, and thermodynamic study, Appl. Water Sci., 7 (2017) 3031–3040.
[40] N. Ayawei, S.S. Angaye, D. Wankasi, E.D. Dikio, Synthesis, characterization and application of Mg/Al layered double hydroxide for the degradation of congo red in aqueous solution, Open J. Phys. Chem., 5 (2015) 56–70.
[41] H.K. Boparai, M. Joseph, D.M. O'Carroll, Kinetics and thermodynamics of cadmium ion removal by adsorption onto nano zerovalent iron particles, J. Hazard. Mater., 186 (2011) 458–465.
[42] O. Çelebi, Ç. Uzum, T. Shahwan, H.N. Erten, A radiotracer study of the adsorption behavior of aqueous Ba^{2+} ions on nanoparticles of zero-valent iron, J. Hazard. Mater., 148 (2007) 761–767.
[43] C. Theivarasu, S. Mylsamy, Removal of malachite green from aqueous solution by activated carbon developed from

cocoa (*Theobroma cacao*) shell: kinetic and equilibrium studies, E-J. Chem., 8 (2011) 363–371.
[44] U. Israel, U.M. Eduok, Biosorption of zinc from aqueous solution using coconut (*Cocos nucifera* L) coir dust, Arch. Appl. Sci. Res., 4 (2012) 809–819.
[45] H. Shahbeig, N. Bagheri, S.A. Ghorbanian, A. Hallajisani, S. Poorkarimi, A new adsorption isotherm model of aqueous solutions on granular activated carbon, World J. Model. Simul., 9 (2013) 243–254.
[46] Y. Pei, D. Guo, Q. An, Z. Xiao, S. Zhai, B. Zhai, Hydrogels with diffusion-facilitated porous network for improved adsorption performance, Korean J. Chem. Eng., 35 (2018) 2384–2393.
[47] E. Augustus, A. Samuel, A. Nimibofa, W. Donbebe, Removal of congo red from aqueous solutions using fly ash modified with hydrochloric acid, Br. J. Appl. Sci. Technol., 20 (2017) 1–7.
[48] F. Brouers, T.J. Al-Musawi, On the optimal use of isotherm models for the characterization of biosorption of lead onto algae, J. Mol. Liq., 212 (2015) 46–51.
[49] J.P. Simonin, On the comparison of pseudo-first order and pseudo-second order rate laws in the modeling of adsorption kinetics, Chem. Eng. J., 300 (2016) 254–263.
[50] L. Largitte, R. Pasquier, A review of the kinetics adsorption models and their application to the adsorption of lead by an activated carbon, Chem. Eng. Res. Des., 109 (2016) 495–504.
[51] N. Sivarajasekar, N. Mohanraj, S. Sivamani, J. Prakash Maran, I. Ganesh Moorthy, K. Balasubramani, Statistical optimization studies on adsorption of ibuprofen onto Albizialebbeck seed pods activated carbon prepared using microwave irradiation, Mater. Today Proc., 5 (2018) 7264–7274.
[52] O. Kutlu, G. Kocar, Upgrading lignocellulosic waste to fuel by torrefaction: characterisation and process optimization by response surface methodology, Int. J. Energy Res., 42 (2018) 1–15.